

# 000 001 002 003 004 005 006 007 008 009 010 011 012 013 014 015 016 017 018 019 020 021 022 023 024 025 026 027 028 029 030 031 032 033 034 035 036 037 038 039 040 041 042 043 044 045 046 047 048 049 050 051 052 053 GRAPH-BASED NEAREST NEIGHBORS WITH DYNAMIC UPDATES VIA RANDOM WALK-BASED ANALYSIS

Anonymous authors

Paper under double-blind review

## ABSTRACT

Approximate nearest neighbor search (ANN) is a common way to retrieve relevant search results, especially now in the context of large language models and retrieval augmented generation. One of the most widely used algorithms for ANN is based on constructing a multi-layer graph over the dataset, called the Hierarchical Navigable Small World (HNSW). While this algorithm supports insertion of new data, it does not support deletion of existing data. Moreover, deletion algorithms described by prior work come at the cost of increased query latency, decreased recall, or prolonged deletion time. In this paper, we propose a new theoretical framework for graph-based ANN based on random walks. We then utilize this framework to analyze a randomized deletion approach that preserves hitting time statistics compared to the graph before deleting the point. We then turn this theoretical framework into a *deterministic* deletion algorithm, and show that it provides better tradeoff between query latency, recall, deletion time, and memory usage through an extensive collection of experiments.

## 1 INTRODUCTION

We study the *approximate nearest neighbor search problem* (ANN): given a collection of  $n$  points  $P \subset \mathbb{R}^d$ , a parameter  $k$  and a query point  $q \in \mathbb{R}^d$ , the goal is to find the top- $k$  points in  $P$  that are closest to  $q$  under some distance measurements such as  $\ell_2$  distance or cosine similarity<sup>1</sup>. This problem is a fundamental component of Retrieval Augmented Generation (RAG), widely adopted to improve the accuracy of Large Language Models (LLM) (Lewis et al., 2020; Gao et al., 2023; Jiang et al., 2023; Fan et al., 2024). One of the most popular ways to solve the ANN problem is through graph-based approaches, where a data-dependent graph is constructed of the dataset, and the queries can be quickly routed on such graph (Jayaram Subramanya et al., 2019; Malkov & Yashunin, 2020; Fu et al., 2019). In this work, we focus on the Hierarchical Navigable Small World (HNSW) graph (Malkov & Yashunin, 2020), a data structure with strong practical performances. This is a multi-layer graph data structure, where the higher layers of the graph tend to have fewer vertices and “long-range” edges that help to navigate between clusters, while the lower layers have “short-range” edges that enhance the connectivity within the clusters. To perform a query search, one starts at the higher layers via the long-range edges to make coarse-grained progress towards the clusters containing the nearest neighbors, and drops to lower layers for finer-grained progress to find the nearest neighbors within the cluster.

While the HNSW algorithm can naturally handle insertions (Harwood et al., 2024), they do not possess *deletion* capabilities. This becomes more and more problematic as modern datasets are highly dynamic and require many deletions. For example, advertisers may remove ads when the campaign budget is exhausted; a clothing retailer may remove spring clothing in the fall and remove fall clothing in the spring; a shoe company may eliminate a previous shoe version when a new generation drops. Thus, deletion is a common and necessary operation.

Since the HNSW algorithm does not come with a deletion procedure, a common, practical approach is to never delete a point at all. Instead, the corresponding vertex in the graph is marked with a “tombstone” indicating that the point should never be outputted as a nearest neighbor. At query time, these tombstones can either be handled in post-processing (the corresponding points would be

<sup>1</sup>In this paper, we use  $\|\cdot\|$  to denote such abstract distance measurement.

removed from the output) or in real-time (modifying the HNSW algorithm to never stop its search at a tombstone). We consider this algorithm as a baseline for our proposed approach. The advantage of this approach is that graph navigability is preserved, and therefore tombstones maintain high recall. However, as tombstones are never removed from the graph, the query latency rises significantly when there are large amounts of tombstones, as the search would take many more steps to reach the desired nearest neighbors. Moreover, the memory usage of the data structure stays constant while the number of points declines, leading to unnecessary storage.

Due to the importance of developing a good deletion algorithm with improved query throughput and memory usage, a rich literature has considered approaches beyond tombstones. An even simpler idea is to delete the point from the graph and the data structure without patching the graph (we will refer to it as a ‘no patching’ algorithm). Such an approach suffers when there are many deletions or queries are drifting towards the clusters being deleted, resulting in much worse recall (Xu et al., 2022). Another class of deletion algorithms is to reconnect the subgraph after deletion as in (Singh et al., 2021; Xu et al., 2022; Xiao et al., 2024; Zhao et al., 2023; Xu et al., 2023; 2025). The reconnection strategy ranges from local to global: if we want to delete  $p$ , a local reconnect attempts to find for every  $u \in N(p)$ , the neighborhood of  $p$ , another point  $v \in N(p)$  that is the nearest neighbor of  $u$ . This approach has low query latency and slightly improved recall compared to no patching, but the recall is still significantly lower than in other alternatives. To further improve recall, Singh et al. (2021) proposes the FreshDiskANN algorithm that uses a 2-hop neighborhood: instead of only rerouting within  $N(p)$ , FreshDiskANN adds edges between  $u$  and  $N(p) \cup N(u)$ , then prunes edges to ensure the sparsity of the graph. A more global approach introduced by Xu et al. (2022) (where they termed the algorithm global reconnect) is to re-insert all the points in  $N(p)$  and improve the connectivity of the subgraph by utilizing the robustness of the HNSW insertion procedure. Both FreshDiskANN and global reconnect suffer from much longer deletion times due to the non-local nature of the algorithm and the need to interact with larger subgraphs, and require nontrivial effort to parallelize the insertions.

**Our results.** Our main contribution is a deletion procedure that arises through a theoretically grounded twin framing of the HNSW algorithm. This algorithm enjoys good recall, query speed, overall deletion time and memory usage, as summarized in Table 1. In the original HNSW algorithm, for a given query  $q$ , the algorithm walks to the adjacent vertex  $u$  that minimizes  $\|q - u\|$ , in a deterministic and greedy fashion. In our twin formulation, we “soften” it by walking to a random neighbor with probability proportional to  $\exp(-r^2 \cdot \|q - u\|^2)$  for  $r > 0$ . We call this a “softmax walk”. While highly similar to the “hard” greedy walk (as we confirm experimentally), this random walk interpretation leads to a theoretical deletion procedure that maintains the properties of the original random walk. Specifically, the algorithm functions by first computing local edge weights over  $N(p)$  that precisely preserve the random walk probability, then using a simple randomized sparsification scheme that approximates the *hitting time* of a walk, i.e., the expected number of steps it takes for a random walk at a vertex  $u$  to reach a vertex  $v$ . While this does not directly guarantee that we will hit the same nearest neighbors exactly, it does ensure that we make a similar number of steps to the target as before. We then turn this randomized, theoretical algorithm into a deterministic, practical algorithm: instead of random sampling edges, we could compute the edge weights first then simply take heaviest edges. We conduct extensive experiments on various datasets in the *mass deletion setting*, where large fraction of the points are removed from the dataset **and show that our method has strong advantage when points are frequently deleted in large batches**. We show the edge of our method over other alternatives in four key metrics: recall, query speed, deletion time and memory usage.

Table 1: Summary of HNSW deletion algorithms.

Method	Recall	Speed	Del Time	Space
Tombstone	✓	✗	✓	✗
No patch	✗	✓	✓	✓
Local	✗	✓	✓	✓
FreshDiskANN	✓	✓	✗	✓
Global	✓	✓	✗	✓
SPatch (ours)	✓	✓	✓	✓

108 

## 2 RELATED WORK

109  
110 **Approximate Nearest Neighbor Search.** Approximate nearest neighbor (ANN) search is a core  
111 algorithmic task with a long line of research, both in theory and in practice. Theoretically, Locality  
112 Sensitive Hashing (LSH) (Indyk & Motwani, 1998; Andoni & Indyk, 2008; Andoni & Razenshteyn,  
113 2015; Andoni et al., 2015; 2017; 2018; Dong et al., 2020) has been a popular solution with provably  
114 fast query time and efficient memory usage. While LSH offers good performance in theory, its  
115 practical variants are usually *data-oblivious*. On the other hand, practical ANN algorithms are  
116 oftentimes *data-dependent*; this class of algorithms includes quantization methods (Jégou et al., 2010;  
117 Ge et al., 2013; Kalantidis & Avrithis, 2014; Yue et al., 2024; Gao & Long, 2024) and graph-based  
118 methods (Malkov & Yashunin, 2020; Jayaram Subramanya et al., 2019; Wang et al., 2021; Fu et al.,  
119 2019; Harwood & Drummond, 2016; Groh et al., 2023), the latter of which are the focus of this work.  
120 In these algorithms, the points in the dataset are coalesced into a specially-constructed proximity  
121 graph. To handle a query, one runs a greedy search algorithm to traverse the graph (i.e., iteratively  
122 move from the current point to its adjacent point closest to the query vector) to find the approximate  
123 nearest neighbors of the query. Among this body of work, we focus on the Hierarchical Navigable  
124 Small World (HNSW) algorithm of Malkov & Yashunin (2020), due to its wide adoption, fast query  
125 throughput, and good recall characteristics. A key limitation of HNSW is that it only explicitly  
126 supports insert and query operations, and implicitly assumes that the dataset is either static or only  
127 incremental. In practice, deletions (if any) are usually handled ad-hoc; the industry standard is to  
128 mark any deleted vectors as unreturnable “tombstones”, and periodically rebuild the data structure  
129 entirely from scratch at great cost (Xu et al., 2022). Some more recent approaches try to directly  
130 incorporate some notion of deletion into the graph data structure, preempting the need for periodic  
131 batch rebuilds (Singh et al., 2021; Xu et al., 2022; Xiao et al., 2024; Xu et al., 2023; Zhao et al.,  
132 2023; Xu et al., 2025). These methods typically operate by first excising the deleted node from the  
133 graph, then “patching” the graph by adding new connections among the removed node’s former  
134 neighborhood. However, most of these approaches offer no theoretical guarantees and typically come  
135 with both performance and recall penalties on real-world datasets, especially for mass deletion.  
136

137 **Graph Sparsification and Random Walks.** Given a graph, an elementary way to explore it is through  
138 random walks, which is both practical (Hamilton et al., 2017) and has rich theoretical connections  
139 to electrical networks (Doyle & Snell, 1984; Tetali, 1991) and spectral graph theory (Chung, 1997;  
140 Spielman, 2007). Important statistics of random walks, including hitting time and commuting  
141 time (Aldous & Fill, 2002) can be computed by solving linear systems in the graph Laplacian  
142 matrix (Merris, 1994). A popular approach to improve the efficiency of solving Laplacian linear  
143 systems is via *spectral sparsification* that reduces the number of edges in the graph while preserving  
144 all Laplacian quadratic forms by sampling according to the effective resistances of edges (Spielman  
145 & Srivastava, 2011; Batson et al., 2009). All state-of-the-art solvers for Laplacian systems utilize  
146 spectral sparsification (Spielman & Teng, 2004; Koutis et al., 2010; Peng & Spielman, 2014; Cohen  
147 et al., 2014; Kyng & Sachdeva, 2016). In this work, we focus on another type of sparsification, based  
148 on sampling by row norms (Drineas & Kannan, 2001; Frieze et al., 2004; Kannan & Vempala, 2017).  
149 It is conceptually simpler and more efficient to implement, though it provides weaker guarantees.  
150

151 

## 3 PRELIMINARIES

152 **HNSW.** The Hierarchical Navigable Small World (HNSW) data structure proposed in Malkov &  
153 Yashunin (2020) is a graph-based ANN data structure that utilizes a *hierarchical* structure. In  
154 particular, it is a sequence of undirected graphs<sup>2</sup> with each graph in the sequence called a “layer”. For  
155 the remainder of this paper, we assume there are  $L$  layers of graphs, with the top one as the  $L$ -th layer  
156 and the bottom one as the 1st layer. The bottom layer of the HNSW contains one vertex for each point  
157 in the dataset, and each other layer contains a random subset of points in the layer below. In addition  
158 to internal edges within a layer, the two vertices representing the same point in two consecutive layers  
159 also have a vertical edge between them so that a search could traverse between layers.  
160

161 The fundamental operation of the HNSW is the search operation. Given a query point  $q$ , the search  
162 starts at the  $L$ -th layer with an entry point. At any timestamp  $t$ , we let  $u_t$  be the point where the query  
163  $q$  is currently on with  $u_0$  being the entry point, then we move  $q$  to  $u_{t+1} := \arg \min_{v \in N(u_t)} \|q - v\|$ .  
164

<sup>2</sup>In some library implementations such as FAISS, directed graphs are used instead.

When the search can no longer make progress, it uses the vertical edge to move one layer down, and repeat the process until the bottom layer. In the remainder of this paper, we refer to this procedure as the “greedy search”. The insertion is then executed by running greedy search on the point-to-be-inserted (with more entry points to move down layers) and add edges along the way. For a more comprehensive overview of HNSW and related algorithms, see Appendix D.

HNSW and other graph-based nearest neighbor search data structures have also been studied through the lens of theory. Laarhoven (2018) studies the performance of greedy search when the size of the dataset  $n = 2^d$ . Fu et al. (2019) analyzes the time and space complexity of searching in the monotonic graphs, and it requires the query to be one of the points in the dataset. Prokhorenkova & Shekhovtsov (2020) proves that the greedy search can be done in sublinear time on the plain nearest neighbor graph in both the dense and sparse regime, and adding vertical edges as in HNSW effectively reduces the number of steps to find the correct nearest neighbor. Shrivastava et al. (2023) relaxes the assumption of nearest neighbor graphs to approximate nearest neighbor graphs. Indyk & Xu (2023) crafts a condition called  $\alpha$ -shortcut reachability, and proves a class of graph-based algorithms are provably efficient for  $\alpha$ -shortcut reachable graphs. Lu et al. (2024) further speeds up the search process by using approximate distances instead of exact distances and proves probabilistic guarantees for this approximation. Diwan et al. (2024) considers a class of simplified HNSW graphs and proves the navigability under certain construction algorithm. Oguri & Matsui (2024) shows that adaptively choosing the entry point provably functions better than using a fixed entry point.

**Deletion Strategies for Graph-based ANN.** One could alternatively interpret HNSW as a multi-layer version of the DiskANN data structure (Jayaram Subramanya et al., 2019), with improved navigability between distant clusters. While these data structures are naturally attuned for insertions, deletion is much more challenging and is heavily based on heuristics. What would be some metrics we’d want a good deletion algorithm to have? 1). Memory usage. We would like the space consumed by the data structure to be proportional to the number of points stored in the data structure; 2). Efficiency. We would like the deletion algorithm to be performed efficiently, and ideally, as efficient as the search algorithm; 3). Recall. The deletion algorithm should not impair the recall performance of the algorithm. If one only cares about the recall, a theoretically “optimal” strategy could be developed:

**Theorem 3.1.** *Let  $P \subset \mathbb{R}^d$  be an  $n$ -point dataset preprocessed by an HNSW and  $p \in P$  be a point to-be-deleted that is not the entry point. Fix a query point  $q \in \mathbb{R}^d$  and suppose the search reaches layer  $l \in \{1, \dots, L\}$ , let  $N(p)$  denote the neighborhood of  $p$  at layer  $l$ . Suppose  $q$  reaches  $N(p)$ , visits and leaves  $p$ . Consider the deletion procedure that removes  $p$  at layer  $l$  and forms a clique over  $N(p)$ , then the search of  $q$  on the new graph is equivalent to the search of  $q$  on the old graph.*

We defer the proof to Appendix C. The above theorem indicates that it is enough to design a data structure that emulates the subgraph without deleting  $p$ . Two obvious choices for an exact data structures are 1). Tombstone, where the subgraph structure is preserved and we will still visit  $p$ ; 2). Clique, where all possible paths in  $N(p)$  are preserved.

These two approaches share similar drawbacks. While the tombstone algorithm cannot ever free memory and reduces query throughput through lengthened walks, the clique algorithm densifies subgraphs and reduces throughput by increasing the number of distance calculations made per step.

## 4 SPATCH: VERTEX DELETION VIA RANDOM WALK PRESERVING SPARSIFICATION

To motivate our deletion algorithm, we develop a theoretical framework for analyzing HNSW that, *instead of walking to the nearest point over the neighborhood, performs a random walk with probability given by the softmax of the squared distance*.

Specifically, let  $q$  be the query point and suppose the search is currently on point  $u$ . Instead of deterministically moving to  $\operatorname{argmin}_{c \in N(u)} \|c - q\|$ , we move to a random  $c \in N(u)$  with probability  $\frac{\exp(-r^2 \cdot \|c - q\|^2)}{\sum_{v \in N(u)} \exp(-r^2 \cdot \|v - q\|^2)}$ . We call this search algorithm the **softmax walk**. While this is different from greedy search, we empirically validate that the performance of the softmax walk for large enough  $r$  is very similar to that of the greedy walk (see Section 5). This simple modification enables us to analyze the graph search from the perspective of a random walk. Instead of interpreting the HNSW graph as an unweighted graph, we can now view it as a *weighted* graph with edge weight

216 determined by the query point  $q$ : letting  $u$  be the point in the graph that the search for  $q$  is currently  
 217 on, for any edge  $\{u, v\}$ , the edge weight is  $w(u, v) = \exp(-r^2 \cdot \|q - v\|^2)$ . The HNSW search then  
 218 performs a random walk on this weighted graph. We could interpret it as a probabilistic HNSW:  
 219

- Instead of greedy search, we use *random walk*;
- Instead of taking the top- $t$  nearest neighbors, we *sample  $t$  edges proportional to edge weights*.

222 The edge weights we choose are equal to the Gaussian kernel between the query and the dataset.  
 223 Intuitively, this is particularly useful to emulate greedy search because it helps differentiate the  
 224 distances: if  $q$  is far away from  $v$ , then  $\exp(-r^2 \cdot \|q - v\|^2)$  would be much smaller than a  $v'$  that is  
 225 closer to  $q$ . Hence, under a proper choice of  $r$ , the Gaussian kernel function assigns exponentially  
 226 high probability to nearby points, emulating the greedy search.

227 We remark that graphs with Gaussian kernel weights are very widely used. Note, however, the  
 228 difference in our case: the weight of an edge  $\{u, v\}$  is not  $\exp(-r^2 \cdot \|u - v\|^2)$  as it would normally  
 229 be, but rather, the edge is viewed as two directed edges  $u \rightarrow v$  and  $v \rightarrow u$ , with respective weights  
 230  $\exp(-r^2 \cdot \|q - v\|^2)$  and  $\exp(-r^2 \cdot \|q - u\|^2)$ . Thus, the edge weight is independent of its source  
 231 point, and varies by the query  $q$  being searched.

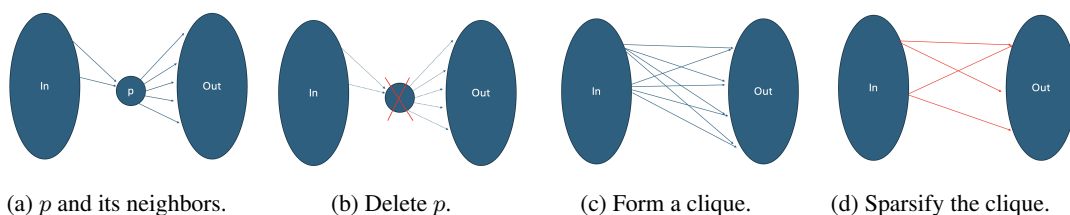
232 Thus, the graph constructed by our twin HNSW formulation can be formally viewed as the result  
 233 of randomized graph sparsification. This algorithm can be integrated into the multi-layer HNSW  
 234 structure by repeating the procedure from layer  $l$  to 0. This weighted graph sparsification perspective  
 235 provides the motivation and theoretical foundation of our deletion algorithm.

236 As discussed in Section 3, we would like a deletion algorithm that is optimized for memory usage,  
 237 efficiency, and recall. Since we are now working with random walks, we first prove a variant of  
 238 Theorem 3.1 in our model: instead of preserving the exact search path after deletion, we aim to  
 239 preserve the random walk probabilities after deletion.

240 **Theorem 4.1.** *Let  $G = (V, E, w)$  be a weighted graph. Define the random walk under the weights  $w$   
 241 for any edge  $\{u, v\} \in E$  as  $\Pr[u \rightarrow v \mid w] = \frac{w(u, v)}{\deg(u)}$  where  $\deg(u) = \sum_{z \in N(u)} w(u, z)$ . Let  $p$  be  
 242 the point to be deleted. For all  $u, v \in N(p)$ , define the new weights  $w'(u, v)$  as  $w'(u, v) = w(u, v) +$   
 243  $\frac{w(u, p) \cdot w(p, v)}{\deg(p)}$ . Let  $E(p) = \{\{u, p\} : u \in N(p)\}$  and  $C(p) = \{\{u, v\} : u \neq v, u, v \in N(p)\}$ . Then  
 244 for the new graph  $G' = (V \setminus \{p\}, E \setminus E(p) \cup C(p), w')$ , we have*

$$\Pr[u \rightarrow v \mid w'] = \Pr[(u \rightarrow p \rightarrow v) \vee (u \rightarrow v) \mid w].$$

245 The proof is deferred to Appendix C. This theorem is known as a “star-mesh transform”, and arises  
 246 from Schur complements and Gaussian elimination (Rosen, 1924; Dorfler & Bullo, 2012; Wagner  
 247 et al., 2018). The new edges  $C(p)$  induce a clique over the neighborhood of  $p$ , making the graph  
 248 denser than before. To sparsify the graph, we adapt a simple strategy: sampling edges according to  
 249 edge weights. The complete algorithm, called **SPatch**: Sparsified Patching, is given in Algorithm 1  
 250 and shown in Figure 1.



261 Figure 1: The deletion procedure of Algorithm 1. It proceeds by first forming a clique over the  
 262 neighborhood of a deleted point, and then sparsifies the clique according to edge weights.

263 To prove theoretical guarantees for Algorithm 1, we need to introduce a few linear algebraic definitions  
 264 related to graphs.

265 **Definition 4.2.** *Let  $G = (V, E, w)$ . Let  $W \in \mathbb{R}^{m \times m}$  be the diagonal matrix for edge weights, and  
 266 let  $B \in \mathbb{R}^{m \times n}$  be the signed edge-vertex incidence matrix, i.e., each row of  $B$  corresponds to an  
 267 edge and it has two nonzero entries on the two endpoints of the edge, with one being +1 and the*

270

**Algorithm 1** SPatch: Sparsified Patching

---

1: **procedure** SPATCH( $G(V, E); p \in V; r, \alpha, t \geq 0$ )  
2:      $\triangleright p$  is the point to be deleted from the graph.  
3:     Define  $w(u, v) = \exp(-r^2 \cdot \|u - v\|^2)$  for all  $u, v$   
4:     Let  $N_{\text{in}}(p)$  be in-neighbors of  $p$  and  $N_{\text{out}}(p)$  be out-neighbors of  $p$   
5:      $t = \alpha \cdot (|N_{\text{in}}(p)| + |N_{\text{out}}(p)|)$   
6:      $\deg(p) = \sum_{u \in N_{\text{in}}(p)} w(u, p) + \sum_{v \in N_{\text{out}}(p)} w(p, v)$   
7:     **for**  $u \in N_{\text{in}}(p)$  and  $v \in N_{\text{out}}(p)$  **do**  
8:          $w'(u, v) = w(u, v) + \frac{w(u, p) \cdot w(p, v)}{\deg(p)}$   $\triangleright$  Compute new weights for all pairs between in- and  
out-neighbors.  
9:     **end for**  
10:     $E' = \{(u, v) : u \in N_{\text{in}}(p), v \in N_{\text{out}}(p), (u, v) \in \text{Top-}\tau(w'(u, v))\}$   
11:     $V \leftarrow V \setminus \{p\}$   $\triangleright$  Delete  $p$  from the graph.  
12:     $E(p) = \{(u, v) : u \in N_{\text{in}}(p), v \in N_{\text{out}}(p)\}$   
13:     $E \leftarrow E \setminus E(p) \cup E'$   $\triangleright$  Remove existing edges from  $N_{\text{in}}(p)$  to  $N_{\text{out}}(p)$ , add edges from  
 $E'$ .  
14: **end procedure**  


---

288

289 other being  $-1$  randomly assigned. The graph Laplacian matrix of  $G$  is defined as  $L = B^\top WB$ .  
290 Equivalently, let  $A \in \mathbb{R}^{n \times n}$  be its weighted adjacency matrix and  $D \in \mathbb{R}^{n \times n}$  be its diagonal degree  
291 matrix, then we have  $L = D - A$ .

292

293 Graph Laplacians are among the most important linear operators associated with graphs, and have a  
294 rich literature (Merris, 1994; Chung, 1997; Spielman, 2007). In the following discussion, we consider  
295 the Laplacian matrix of the clique over  $N(p)$ . Sparsifying by edge weights is equivalent to sparsifying  
296 by the *squared row norms* of  $\sqrt{WB}$ , which provides an additive error approximation in terms of the  
297 Frobenius norm (Drineas & Kannan, 2001; Frieze et al., 2004; Kannan & Vempala, 2017).

298

299 **Theorem 4.3.** Let  $G = (V, E, w)$  and  $L \in \mathbb{R}^{n \times n}$  be its Laplacian matrix. Let  $\varepsilon \in (0, 1)$ . Suppose  
300 we generate a matrix  $\tilde{C} \in \mathbb{R}^{s \times n}$  by sampling each row of  $\sqrt{WB}$  proportionally to its squared row  
301 norm with  $s = 200\varepsilon^{-2}$ , and reweight row  $i$  by  $1/(p_i s)$  where  $p_i = \|(\sqrt{WB})_{i,*}\|_2^2 / \|\sqrt{WB}\|_F^2$ . Then  
with probability at least 0.99,  $\|\tilde{C}^\top \tilde{C} - L\|_F \leq \varepsilon \cdot \text{tr}[W]$ , where  $\text{tr}[W]$  is the trace of matrix  $W$ .

302

303 The proof is deferred to Appendix C. Since Theorem 4.3 sparsifies the graph by sampling edges, the  
304 resulting matrix  $\tilde{C}^\top \tilde{C}$  also forms a weighted graph, which we denote by  $G' = (V, E', w')$ . Compared  
305 to the standard spectral sparsification of graphs (Spielman & Srivastava, 2011), our sparsification  
306 scheme does not necessarily preserve the *connectivity* of the resulting graph  $G'$ . Intuitively, sampling  
307 by edge weights is likely to ensure a cluster of close points to be well-connected, but it falls short when  
308 there are intercluster edges with small edge weights. However, we only perform the sparsification  
309 process on the *bottom layer* of HNSW, whose role is to search through edges within a cluster, after  
310 intercluster connections have been effectively handled by top layers. This is also confirmed by our  
311 experiments (see Section 5). Hence, we assume the sparsified graph  $G'$  remains connected.

311

312 What does a Frobenius norm error approximation of the Laplacian imply for random walks? We  
313 prove that it approximately preserves the *hitting time* of the random walk.

314

315 **Definition 4.4.** Let  $G = (V, E, w)$  be a graph and  $u, v \in V$ . The hitting time from  $u$  to  $v$ , denoted  
316 by  $h_G(u, v)$ , is the expected number of steps for a random walk starting at  $u$  to reach  $v$ . When  $G$  is  
clear from context, we denote it by  $h(u, v)$ .

317

318 Our main result is that an additive Frobenius norm error approximation of Laplacian gives a  
319 multiplicative-additive error approximation on the hitting time.

320

321 **Theorem 4.5** (Informal version of Theorem B.8). Let  $G = (V, E, w)$  be a graph, let  $G' = (V, E', w')$   
322 be the graph induced by Theorem 4.3, and suppose  $G'$  is connected. Let  $d_{\min}, d_{\max}$  be the min and  
323 max degree of  $G$ , and let  $\phi(G)$  be the edge expansion of the graph  $G$ . For any  $u \neq v \in V$ ,

324

$$|h_G(u, v) - h_{G'}(u, v)| \leq \frac{\varepsilon \text{tr}[W]}{d_{\min}} h_G(u, v) + \varepsilon \text{tr}[W]^2 \left( \frac{\phi(G)^2}{d_{\max}} - \varepsilon \text{tr}[W] \right)^{-2}$$

324 holds with probability at least 0.99, where  $\phi(G) = \min_{S \subseteq V} \frac{\sum_{u \sim v, u \in S, v \notin S} w(u, v)}{\min\{|S|, |V| - |S|\|}$ .  
 325

326 If our softmax walk algorithm was to perform its random walk without stopping at local minima, then  
 327 Theorem 4.5 would say that if  $u$  is the entry point and  $v$  is the desired destination, then the expected  
 328 numbers of steps to reach  $v$  from  $u$  before and after sparsification are similar. However, the softmax  
 329 walk stops at local minima, therefore, a bound on hitting time *does not* imply the walk could hit the  
 330 correct destinations. Our experiments (Section 5) suggest that instead of directly correlating to the  
 331 correctness of the algorithm, hitting time is a good proxy when designing the sparsification algorithm,  
 332 as Algorithm 1 has good recall, query speed, deletion time, and memory utilization.

333 Theorem 4.3 states that to obtain an additive Frobenius norm error of  $\varepsilon \cdot \text{tr}[W]$ , we need to sample  
 334  $O(\varepsilon^{-2})$  edges, and this in turn provides an error bound on the hitting time per Theorem 4.5. How  
 335 many edges do we need to sample in order to minimize the overall error? We show that in two  
 336 common settings, the number of edges is linear in the number of points,  $|N(p)|$ :

337 **Corollary 4.6.** *Let  $G = (V, E, w)$  be a weighted complete graph with  $|V| = n$  and  $G' = (V, E', w')$   
 338 be the induced graph by applying Theorem 4.3 to  $G$ . If  $|E'| = O(\max_{u, v \in N(p)} h_G(u, v) \cdot n)$ , then  
 339 with probability at least 0.99, for any  $u, v \in V$ ,  $|h_G(u, v) - h_{G'}(u, v)| \leq \sqrt{n \cdot h_G(u, v)}$ . given one  
 340 of the two settings:*

- 342 • *Single cluster: for any  $u, v \in V$ ,  $w(u, v) = O(1)$ ;*
- 343 • *Many small clusters: there are  $\sqrt{n}$  clusters of size  $\sqrt{n}$ . Within each cluster, the edge weights are  
 344  $O(1)$ , and between clusters, the edge weights are  $O(1/n)$ .*

345 **From Random Sampling to Top- $t$  Selection.** In essence, the SPatch framework suggests a  
 346 novel approach for performing local reconnect: instead of using the distances between points in  
 347  $N(p)$  directly, one should incorporate the distance between  $N(p)$  and  $p$  as well. This offers a  
 348 natural transition to a more practical and efficient *deterministic* deletion algorithm: first compute  
 349 the new local edge weights  $w'(u, v)$  for all  $u, v \in N(p)$ , then keep the top- $t$  edges with the largest  
 350 weights. Note that for large enough  $r$ , the probability of sampling edges outside of the top- $t$  edges is  
 351 exponentially small. Thus, we could safely replace the “sample  $t$  edges” step with “keep the top- $t$   
 352 edges with largest weights”. This switch offers several practical advantages: in general, computing the  
 353 edge weights then selecting the top- $t$  heaviest edges is more efficient than sampling  $t$  edges without  
 354 replacement. Thus, all our experiments are performed with the deterministic deletion algorithm.

## 355 5 EXPERIMENTS

356 We conduct extensive experiments to test the practical performance of our deletion algorithm. In  
 357 the following, we will give a preliminary overview of the experimental setups, then we focus on  
 358 discussing two sets of experiments: the major focus is on a *mass deletion experiment* where points  
 359 are gradually deleted with no new points inserted. We wrap up the experiment by showing that  
 360 the random walk search algorithm performs as well as the HNSW greedy search. Due to space  
 361 constraints, we defer more details to Appendix E.

### 362 5.1 SETUP

363 **Hardware.** All experiments run on 8x3.7 GHz AMD EPYC 7R13 cores with 64 GiB RAM.

364 **Implementation.** We implement the HNSW data structure by utilizing the FAISS library (Johnson  
 365 et al., 2019; Douze et al., 2024). In particular, we construct the HNSW graph by invoking the  
 366 HNSWFlatIndex of FAISS with the degree parameter  $m = 32$ . We then extract the resulting  
 367 graphs, which are directed, and convert them into a sequence of undirected networkx graphs (Hag-  
 368 berg et al., 2008) for our deletion operations.

369 **Datasets.** We use 4 datasets for our ANN benchmarks: SIFT (Jégou et al., 2011), GIST (Sand-  
 370 hawalia & Jégou, 2010), and one embedding of the MS MARCO (Bajaj et al., 2016) dataset with each  
 371 of MPNet (Song et al., 2020) and MiniLM (Wang et al., 2020). All of the datasets contain 1M points,  
 372 with dimensions 768 (MPNet), 128 (SIFT), 960 (GIST) and 384 (MiniLM).

373 **Deletion algorithm.** For all deletion algorithms, we adopt the strategy that uses the tombstone for all  
 374 top layers and only performs the deletion at the bottom layer. This is viable as the bottom layer is

378 much more connected and denser than all top layers. For `SPatch`, we implement a modified version  
 379 in the following aspects: 1). Since the graph is directed, we let  $L$  be the set of in-neighbors of  $p$  and  
 380 let  $R$  be the set of out-neighbors, for each  $u \in R$ , we pick the top- $t := \alpha \cdot \lceil \frac{|L|+|R|}{|R|} \rceil$  points  $v \in L$   
 381 where  $w'(u, v)$  is maximized. 2). Instead of replacing all edges in  $N(p)$  including those exist before  
 382 deleting  $p$ , we continue to add new edges with large weights until all top- $t$  edges are added. This  
 383 slightly densifies the graph without adding many edges.  
 384

385 **Evaluation metrics.** We focus on four important evaluation metrics: top-10 recall (defined as  
 386 the fraction of top-10 nearest neighbors returned by the data structure over the top-10 true nearest  
 387 neighbors), number of distance computations for queries, the total time for deletion and the number  
 388 of edges at the bottom layer. We use the number of distance computations as a metric for query  
 389 throughput because for either the greedy search or random walk-based search, the main runtime  
 390 bottleneck is the number of distance computations. For deletion procedure, as it involves more  
 391 complicated operations such as computing edge weights for a clique, we directly measure the overall  
 392 runtime of deletion. Finally, we use the number of edges at the bottom layer as a proxy measurement  
 393 for the memory/space usage of the deletion algorithm, and in Appendix E.3 in particular Figure 7, we  
 394 show that it directly corresponds to the reduction in empirical memory utilization.  
 395

## 5.2 DELETION EXPERIMENT

396 In this experiment, we evaluate the performance of our deletion algorithm under the mass deletion  
 397 setting, as follows: In total 80% of the points will be removed from the dataset, for which every 0.8%  
 398 of the points being deleted, we run the query through the remaining dataset and record the following  
 399 4 metrics: top-10 recall, number of distance computations, overall deletion time and the number  
 400 of edges at the bottom layer. For the query phase, we randomly pick 5,000 query points for `SIFT`,  
 401 `MPNet`, `Minilm` and 1,000 query points for `GIST`. These queries are fixed throughout the process.  
 402

403 We compare our algorithm against several popular deletion prototypes for HNSW: 1). No patching,  
 404 where the point is deleted from the graph without rerouting or adding any new edges. 2). Tombstone,  
 405 where the point to be deleted is marked as a tombstone vertex without being deleted, and subsequent  
 406 queries do not get stuck at a tombstone vertex. Xu et al. (2023) adapts a version of tombstone with  
 407 periodical scan and merge to ensure the freshness of the index. 3). Local reconnect (Xu et al., 2022),  
 408 where for each point in  $N(p)$ , an edge to its nearest neighbor in  $N(p)$  is added; 4). 2-hop reconnect,  
 409 where the points  $u \in N(p)$  are rerouted to  $N(p) \cup N(u)$  then pruned. A wide array of deletion  
 410 algorithms fall into this category, including Singh et al. (2021); Xu et al. (2023); Zhao et al. (2023);  
 411 Xiao et al. (2024); Xu et al. (2025). We implement and test the FreshDiskANN primitive (Singh et al.,  
 412 2021). We also consider a periodic rebuild strategy: every batch, we rebuild the HNSW from scratch.  
 413

414 We examine Figure 2 method by method.

- 415 • While Tombstone has the best recall among all methods as per Theorem 3.1 (even better than  
 416 periodic rebuild), it quickly falls short in terms of query speed (2.5–3× more distance computations  
 417 than `SPatch`) and its memory usage stays constant as more points are deleted;
- 418 • Recall degrades most quickly when we do not patch, despite its fast query speed, deletion time and  
 419 low memory consumption;
- 420 • Local reconnect has slightly improved recall compared to no patching, yet still worse than others;
- 421 • FreshDiskANN has better recall for datasets such as `SIFT` and `MPNet`, but the deletion time is  
 422 slower. Although it might be suitable when deletions are rare, in the setting of frequent deletions it  
 423 is inefficient. We also include Figure 5 for a deletion time comparison without FreshDiskANN;
- 424 • `SPatch` gives the best *overall* performance among various tradeoffs. While its recall is slightly  
 425 lower than periodic rebuild and Tombstone, its query speed is much faster and memory usage  
 426 decreases as more points are deleted than Tombstone. `SPatch` performs deletion much faster than  
 427 FreshDiskANN and periodic rebuild.

## 5.3 RANDOM SOFTMAX WALK VS. GREEDY SEARCH

428 To empirically substantiate the validity of our randomized “twin” formulation of HNSW, we compare  
 429 the two variants (softmax vs. greedy walk) in Table 2. The results show that they are highly similar  
 430 empirically in recall and throughput, with the softmax variant incurring only a slight loss. This  
 431 validates our use of it as a theoretical model for HNSW.

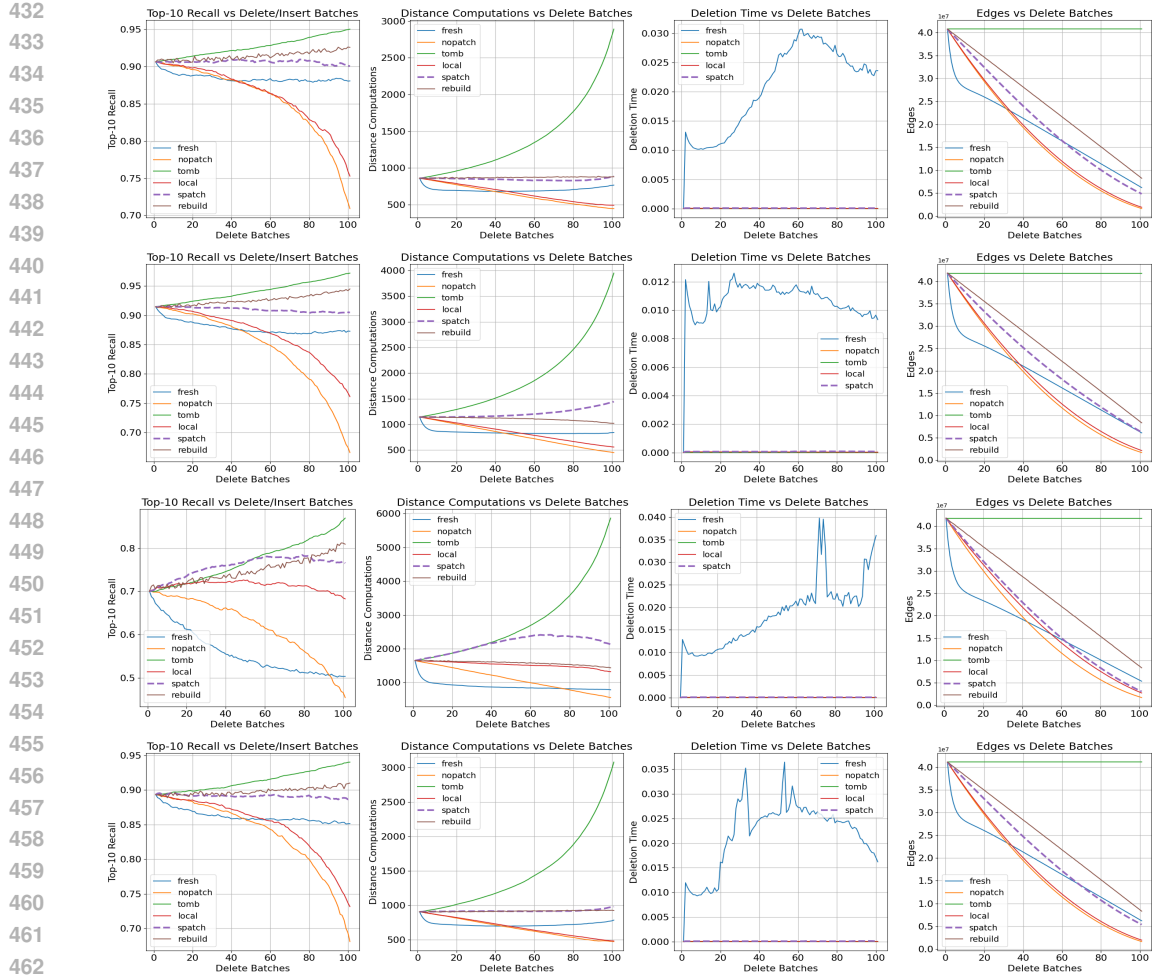


Figure 2: The rows are MPNet, SIFT, GIST and MiniLM, the columns are top-10 recall, number of distance computations per query, total deletion time and number of edges in the bottom layer of the graph. Legends: spatch – our algorithm SPatch, fresh – FreshDiskANN, tomb – tombstone, nopath – no patching, local – local reconnect. For MPNet: we also include rebuild without plotting its deletion time..

Dataset	Top-10 Recall		Distance Computations	
	Softmax	Greedy	Softmax	Greedy
MPNet	89.98%	91.60%	1562	1722
SIFT	91.13%	91.95%	1049	1109
GIST	71.38%	72.46%	1606	1653
MiniLM	89.27%	90.09%	1708	1802

Table 2: Comparison of softmax walk to greedy walk.

## 6 CONCLUSION

In this work, we provide a theoretical framework for HNSW using random walks and sampling. We then propose a deletion algorithm, SPatch, based on a deterministic implementation of the theoretical motivation. Theoretical guarantees and empirical evidence demonstrate that SPatch has good recall, speed, deletion time and memory. This random walk interpretation opens up new opportunities to study HNSW through the lens of random walks. We hope this framework sheds light on more theoretical investigations of HNSW and inspires novel practical algorithms.

486  
487  
ETHICS STATEMENT488  
489  
This work designs fundamental algorithms for ANN data structures with experiments performed on  
490  
standard datasets. We don't foresee any potential ethics concerns of our work.491  
492  
REPRODUCIBILITY STATEMENT493  
494  
This work consists both theoretical and empirical results, we include the proofs of all theoretical  
495  
results in Appendix C, and for empirical results, we will open source the code upon publication of  
496  
this work.497  
498  
REFERENCES499  
500  
David Aldous and James Allen Fill. *Reversible Markov Chains and Random Walks on Graphs*. 2002.  
501  
Unfinished monograph, available at <http://www.stat.berkeley.edu/~aldous/RWG/book.html>.502  
503  
Alexandr Andoni and Piotr Indyk. Near-optimal hashing algorithms for approximate nearest neighbor  
504  
in high dimensions. *Commun. ACM*, 51(1):117–122, January 2008. ISSN 0001-0782.505  
506  
Alexandr Andoni and Ilya Razenshteyn. Optimal data-dependent hashing for approximate near  
507  
neighbors. In *Proceedings of the Forty-Seventh Annual ACM Symposium on Theory of Computing*,  
508  
STOC '15, pp. 793–801, New York, NY, USA, 2015. Association for Computing Machinery.509  
510  
Alexandr Andoni, Piotr Indyk, Thijs Laarhoven, Ilya Razenshteyn, and Ludwig Schmidt. Practical  
511  
and optimal lsh for angular distance. In *Proceedings of the 29th International Conference on*  
512  
*Neural Information Processing Systems - Volume 1*, NIPS'15, pp. 1225–1233, Cambridge, MA,  
513  
USA, 2015. MIT Press.514  
515  
Alexandr Andoni, Thijs Laarhoven, Ilya Razenshteyn, and Erik Waingarten. Optimal hashing-based  
516  
time-space trade-offs for approximate near neighbors. In *Proceedings of the Twenty-Eighth Annual*  
517  
*ACM-SIAM Symposium on Discrete Algorithms*, SODA '17, pp. 47–66, USA, 2017. Society for  
518  
Industrial and Applied Mathematics.519  
520  
Alexandr Andoni, Piotr Indyk, and Ilya Razenshteyn. Approximate nearest neighbor search in high  
521  
dimensions. In *Proceedings of the International Congress of Mathematicians: Rio de Janeiro*  
522  
2018, pp. 3287–3318. World Scientific, 2018.523  
524  
Payal Bajaj, Daniel Campos, Nick Craswell, Hoa Dang, Jianfeng Gao, Xiaodong Liu, Ryan McNa-  
525  
mara, Bhaskar Mitra, Tri Nguyen, Lin Qian, et al. Ms marco: A human generated machine reading  
526  
comprehension dataset. *arXiv preprint arXiv:1611.09268*, 2016.527  
528  
Joshua D. Batson, Daniel A. Spielman, and Nikhil Srivastava. Twice-ramanujan sparsifiers. In  
529  
*Proceedings of the Forty-First Annual ACM Symposium on Theory of Computing*, STOC '09, pp.  
530  
255–262, New York, NY, USA, 2009. Association for Computing Machinery.531  
532  
Jeff Cheeger. *A Lower Bound for the Smallest Eigenvalue of the Laplacian*, pp. 195–200. Princeton  
533  
University Press, Princeton, 1971.534  
535  
Fan R. K. Chung. *Spectral Graph Theory*. American Mathematical Society, Providence, RI, 1997.  
536  
ISBN 978-0-8218-0315-8.537  
538  
Michael B. Cohen, Rasmus Kyng, Gary L. Miller, Jakub W. Pachocki, Richard Peng, Anup B. Rao,  
539  
and Shen Chen Xu. Solving SDD linear systems in nearly  $m \log^{1/2} n$  time. In *Proceedings of the*  
540  
*Forty-Sixth Annual ACM Symposium on Theory of Computing*, STOC '14, pp. 343–352, New York,  
541  
NY, USA, 2014. Association for Computing Machinery.542  
543  
Haya Diwan, Jinrui Gou, Cameron N Musco, Christopher Musco, and Torsten Suel. Navigable graphs  
544  
for high-dimensional nearest neighbor search: Constructions and limits. In *The Thirty-eighth*  
545  
*Annual Conference on Neural Information Processing Systems*, 2024.

540 Yihe Dong, Piotr Indyk, Ilya Razenshteyn, and Tal Wagner. Learning space partitions for nearest  
 541 neighbor search. In *International Conference on Learning Representations*, 2020.

542

543 Florian Dorfler and Francesco Bullo. Kron reduction of graphs with applications to electrical networks.  
 544 *IEEE Transactions on Circuits and Systems I: Regular Papers*, 60(1):150–163, 2012.

545

546 Matthijs Douze, Alexandr Guzhva, Chengqi Deng, Jeff Johnson, Gergely Szilvassy, Pierre-Emmanuel  
 547 Mazaré, Maria Lomeli, Lucas Hosseini, and Hervé Jégou. The faiss library. *arXiv preprint*  
 548 *arXiv:2401.08281*, 2024.

549

550 Peter G. Doyle and J. Laurie Snell. *Random Walks and Electric Networks*, volume 22 of *Carus  
 551 Mathematical Monographs*. Mathematical Association of America, Washington, DC, 1984.

552

553 P. Drineas and R. Kannan. Fast monte-carlo algorithms for approximate matrix multiplication. In  
 554 *Proceedings 42nd IEEE Symposium on Foundations of Computer Science*, pp. 452–459, 2001.

555

556 Wenqi Fan, Yujian Ding, Liangbo Ning, Shijie Wang, Hengyun Li, Dawei Yin, Tat-Seng Chua, and  
 557 Qing Li. A survey on rag meeting llms: Towards retrieval-augmented large language models. In  
 558 *Proceedings of the 30th ACM SIGKDD Conference on Knowledge Discovery and Data Mining*,  
 559 KDD ’24, pp. 6491–6501, New York, NY, USA, 2024. Association for Computing Machinery.  
 560 ISBN 9798400704901.

561

562 Alan Frieze, Ravi Kannan, and Santosh Vempala. Fast monte-carlo algorithms for finding low-rank  
 563 approximations. *J. ACM*, pp. 1025–1041, November 2004.

564

565 Cong Fu, Chao Xiang, Changxu Wang, and Deng Cai. Fast approximate nearest neighbor search  
 566 with the navigating spreading-out graph. *Proceedings of the VLDB Endowment*, 12(5), 2019.

567

568 Jianyang Gao and Cheng Long. Rabitq: Quantizing high-dimensional vectors with a theoretical  
 569 error bound for approximate nearest neighbor search. In *Proceedings of the 2024 ACM SIGMOD  
 570 International Conference on Management of Data*. ACM, 2024.

571

572 Yunfan Gao, Yun Xiong, Xinyu Gao, Kangxiang Jia, Jinliu Pan, Yuxi Bi, Yi Dai, Jiawei Sun, Meng  
 573 Wang, and Haofen Wang. Retrieval-augmented generation for large language models: A survey.  
 574 *arXiv preprint arXiv:2312.10997*, 2023.

575

576 Tiezheng Ge, Kaiming He, Qifa Ke, and Jian Sun. Optimized product quantization for approximate  
 577 nearest neighbor search. In *Proceedings of the IEEE Conference on Computer Vision and Pattern  
 578 Recognition (CVPR)*, pp. 2946–2953. IEEE, 2013.

579

580 Fabian Groh, Lukas Ruppert, Patrick Wieschollek, and Hendrik P. A. Lensch. Ggnn: Graph-based  
 581 gpu nearest neighbor search. *IEEE Transactions on Big Data*, 9(1):267–279, 2023.

582

583 Aric Hagberg, Pieter J. Swart, and Daniel A. Schult. Exploring network structure, dynamics, and  
 584 function using networkx. In *Proceedings of the 7th Python in Science Conference (SciPy2008)*.  
 585 Los Alamos National Laboratory (LANL), Los Alamos, NM (United States), 01 2008.

586

587 William L. Hamilton, Rex Ying, and Jure Leskovec. Inductive representation learning on large graphs.  
 588 In *Proceedings of the 31st International Conference on Neural Information Processing Systems*,  
 589 NIPS’17, pp. 1025–1035, Red Hook, NY, USA, 2017. Curran Associates Inc.

590

591 Ben Harwood and Tom Drummond. Fanng: Fast approximate nearest neighbour graphs. In *Proceed-  
 592 ings of the IEEE Conference on Computer Vision and Pattern Recognition (CVPR)*, pp. 5713–5722.  
 593 IEEE, 2016.

594

595 Ben Harwood, Amir Dezfouli, Iadine Chades, and Conrad Sanderson. Approximate nearest neighbour  
 596 search on dynamic datasets: An investigation, 2024.

597

598 Nico Hezel, Kai Uwe Barthel, Bruno Schilling, Konstantin Schall, and Klaus Jung. Dynamic  
 599 exploration graph: a novel approach for efficient nearest neighbor search in evolving multimedia  
 600 datasets. In *International Conference on Multimedia Modeling*, pp. 333–347. Springer, 2025.

601

602 Piotr Indyk and Rajeev Motwani. Approximate nearest neighbors: towards removing the curse of  
 603 dimensionality. In *Proceedings of the thirtieth annual ACM symposium on Theory of computing*,  
 604 pp. 604–613, 1998.

594 Piotr Indyk and Hsueh-Chia Chen. Worst-case performance of popular approximate nearest neighbor  
 595 search implementations: guarantees and limitations. In *Proceedings of the 37th International*  
 596 *Conference on Neural Information Processing Systems*, NIPS '23, Red Hook, NY, USA, 2023.  
 597 Curran Associates Inc.

598 Suhas Jayaram Subramanya, Fnu Devvrit, Harsha Vardhan Simhadri, Ravishankar Krishnawamy,  
 599 and Rohan Kadekodi. Diskann: Fast accurate billion-point nearest neighbor search on a single  
 600 node. In H. Wallach, H. Larochelle, A. Beygelzimer, F. d'Alché-Buc, E. Fox, and R. Garnett (eds.),  
 601 *Advances in Neural Information Processing Systems*, volume 32. Curran Associates, Inc., 2019.

602 Zhengbao Jiang, Frank Xu, Luyu Gao, Zhiqing Sun, Qian Liu, Jane Dwivedi-Yu, Yiming Yang, Jamie  
 603 Callan, and Graham Neubig. Active retrieval augmented generation. In *Proceedings of the 2023*  
 604 *Conference on Empirical Methods in Natural Language Processing*, pp. 7969–7992, Singapore,  
 605 December 2023. Association for Computational Linguistics.

606 Jeff Johnson, Matthijs Douze, and Hervé Jégou. Billion-scale similarity search with GPUs. *IEEE*  
 607 *Transactions on Big Data*, 7(3):535–547, 2019.

608 Hervé Jégou, Matthijs Douze, and Cordelia Schmid. Product quantization for nearest neighbor search.  
 609 *IEEE transactions on pattern analysis and machine intelligence*, 33(1):117–128, 2010.

610 Hervé Jégou, Romain Tavenard, Matthijs Douze, and Laurent Amsaleg. Searching in one billion  
 611 vectors: Re-rank with source coding. In *2011 IEEE International Conference on Acoustics, Speech*  
 612 *and Signal Processing (ICASSP)*, pp. 861–864, 2011.

613 Yannis Kalantidis and Yannis Avrithis. Locally optimized product quantization for approximate  
 614 nearest neighbor search. In *Proceedings of the IEEE Conference on Computer Vision and Pattern*  
 615 *Recognition (CVPR)*, pp. 2321–2328. IEEE, 2014.

616 Ravindran Kannan and Santosh Vempala. Randomized algorithms in numerical linear algebra. *Acta*  
 617 *Numerica*, 26:95–135, 2017.

618 Ioannis Koutis, Gary L. Miller, and Richard Peng. Approaching optimality for solving sdd linear  
 619 systems. In *2010 IEEE 51st Annual Symposium on Foundations of Computer Science*, pp. 235–244,  
 620 2010.

621 Rasmus Kyng and Sushant Sachdeva. Approximate Gaussian Elimination for Laplacians - Fast,  
 622 Sparse, and Simple . In *2016 IEEE 57th Annual Symposium on Foundations of Computer Science*  
 623 (*FOCS*), Los Alamitos, CA, USA, October 2016. IEEE Computer Society.

624 Thijs Laarhoven. Graph-Based Time-Space Trade-Offs for Approximate Near Neighbors. In Bettina  
 625 Speckmann and Csaba D. Tóth (eds.), *34th International Symposium on Computational Geometry*  
 626 (*SoCG 2018*), Leibniz International Proceedings in Informatics (LIPIcs), pp. 57:1–57:14, Dagstuhl,  
 627 Germany, 2018. Schloss Dagstuhl – Leibniz-Zentrum für Informatik. ISBN 978-3-95977-066-8.

628 Patrick Lewis, Ethan Perez, Aleksandra Piktus, Fabio Petroni, Vladimir Karpukhin, Naman Goyal,  
 629 Heinrich Küttler, Mike Lewis, Wen tau Yih, Tim Rocktäschel, Sebastian Riedel, and Douwe  
 630 Kiela. Retrieval-augmented generation for knowledge-intensive nlp tasks. In *Advances in Neural*  
 631 *Information Processing Systems*, 2020.

632 Kejing Lu, Chuan Xiao, and Yoshiharu Ishikawa. Probabilistic routing for graph-based approximate  
 633 nearest neighbor search. In *Proceedings of the 41st International Conference on Machine Learning*,  
 634 ICML'24. JMLR.org, 2024.

635 Yu A. Malkov and D. A. Yashunin. Efficient and robust approximate nearest neighbor search using  
 636 hierarchical navigable small world graphs. *IEEE Trans. Pattern Anal. Mach. Intell.*, 42(4), 2020.

637 Russell Merris. Laplacian matrices of graphs: a survey. *Linear algebra and its applications*, 197:  
 638 143–176, 1994.

639 Yutaro Oguri and Yusuke Matsui. Theoretical and empirical analysis of adaptive entry point selection  
 640 for graph-based approximate nearest neighbor search, 2024.

648 Richard Peng and Daniel A. Spielman. An efficient parallel solver for sdd linear systems. In *Proceedings of the Forty-Sixth Annual ACM Symposium on Theory of Computing*, STOC '14, pp. 333–342,  
 649 New York, NY, USA, 2014. Association for Computing Machinery. ISBN 9781450327107.

650

651 Liudmila Prokhorenkova and Aleksandr Shekhovtsov. Graph-based nearest neighbor search: from  
 652 practice to theory. In *Proceedings of the 37th International Conference on Machine Learning*,  
 653 ICML'20. JMLR.org, 2020.

654

655 A Rosen. A new network theorem. *Journal of the institution of electrical engineers*, 62(335):916–918,  
 656 1924.

657

658 Harsimrat Sandhawalia and Hervé Jégou. Searching with expectations. In *Proceedings of the  
 659 19th ACM International Conference on Information and Knowledge Management (CIKM)*, pp.  
 660 1997–2000. ACM, 2010.

661

662 Anshumali Shrivastava, Zhao Song, and Zhaozhuo Xu. A theoretical analysis of nearest neighbor  
 663 search on approximate near neighbor graph, 2023.

664

665 Aditi Singh, Suhas Jayaram Subramanya, Ravishankar Krishnaswamy, and Harsha Vardhan Simhadri.  
 666 Freshdiskann: A fast and accurate graph-based ann index for streaming similarity search, 2021.

667

668 Kaitao Song, Xu Tan, Tao Qin, Jianfeng Lu, and Tie-Yan Liu. Mpnet: Masked and permuted  
 669 pre-training for language understanding. In *Advances in Neural Information Processing Systems  
 (NeurIPS)*, 2020.

670

671 Daniel A. Spielman. Spectral graph theory and its applications. In *Proceedings of the 48th Annual  
 672 IEEE Symposium on Foundations of Computer Science (FOCS)*, pp. 29–38. IEEE, 2007. doi:  
 10.1109/FOCS.2007.66.

673

674 Daniel A Spielman and Nikhil Srivastava. Graph sparsification by effective resistances. *SIAM Journal  
 675 on Computing*, 40(6):1913–1926, 2011.

676

677 Daniel A. Spielman and Shang-Hua Teng. Nearly-linear time algorithms for graph partitioning,  
 678 graph sparsification, and solving linear systems. In *Proceedings of the Thirty-Sixth Annual  
 679 ACM Symposium on Theory of Computing*, STOC '04, pp. 81–90, New York, NY, USA, 2004.  
 Association for Computing Machinery.

680

681 Prasad Tetali. Random walks and the effective resistance of networks. *Journal of Theoretical  
 682 Probability*, 4(1):101–109, 1991.

683

684 Tal Wagner, Sudipto Guha, Shiva Kasiviswanathan, and Nina Mishra. Semi-supervised learning on  
 685 data streams via temporal label propagation. In *International Conference on Machine Learning*,  
 pp. 5095–5104. PMLR, 2018.

686

687 Mengzhao Wang, Xiaoliang Xu, Qiang Yue, and Yuxiang Wang. A comprehensive survey and  
 688 experimental comparison of graph-based approximate nearest neighbor search. *arXiv preprint  
 689 arXiv:2101.12631*, 2021.

690

691 Wenhui Wang, Furu Wei, Li Dong, Hangbo Bao, Nan Yang, and Ming Zhou. MiniLM: Deep  
 692 self-attention distillation for task-agnostic compression of pre-trained transformers. *Advances in  
 693 Neural Information Processing Systems*, 33:5776–5788, 2020.

694

695 Per-Åke Wedin. Perturbation theory for pseudo-inverses. *BIT Numerical Mathematics*, 13(2):  
 217–232, 1973.

696

697 H. Weyl. Das asymptotische Verteilungsgesetz der Eigenwerte linearer partieller Differentialgleichungen  
 698 (mit einer Anwendung auf die Theorie der Hohlraumstrahlung). *Mathematische Annalen*, 71:  
 699 441–479, 1912.

700

701 Wentao Xiao, Yueyang Zhan, Rui Xi, Mengshu Hou, and Jianming Liao. Enhancing hnsw index for  
 702 real-time updates: Addressing unreachable points and performance degradation. *arXiv preprint  
 703 arXiv:2407.07871*, 2024.

702 Haike Xu, Magdalen Dobson Manohar, Philip A. Bernstein, Badrish Chandramouli, Richard Wen,  
703 and Harsha Vardhan Simhadri. In-place updates of a graph index for streaming approximate nearest  
704 neighbor search. *arXiv preprint arXiv:2502.13826*, 2025.

705  
706 Yuming Xu, Hengyu Liang, Jin Li, Shuotao Xu, Qi Chen, Qianxi Zhang, Cheng Li, Ziyue Yang,  
707 Fan Yang, Yuqing Yang, Peng Cheng, and Mao Yang. Spfresh: Incremental in-place update for  
708 billion-scale vector search. In *Proceedings of the 27th USENIX Symposium on Operating Systems  
709 Principles (SOSP 2023)*, 2023.

710 Zhaozhuo Xu, Weijie Zhao, Shulong Tan, Zhixin Zhou, and Ping Li. Proximity graph maintenance  
711 for fast online nearest neighbor search, 2022.

712  
713 Qiang Yue, Xiaoliang Xu, Yuxiang Wang, Yikun Tao, and Xuliyuan Luo. Routing-guided learned  
714 product quantization for graph-based approximate nearest neighbor search. In *Proceedings of the  
715 40th IEEE International Conference on Data Engineering (ICDE)*, pp. 4870–4883. IEEE, 2024.

716 Xi Zhao, Yao Tian, Kai Huang, Bolong Zheng, and Xiaofang Zhou. Towards efficient index  
717 construction and approximate nearest neighbor search in high-dimensional spaces. *Proceedings  
718 of the VLDB Endowment*, 16(8):1979–1991, 2023. doi: 10.14778/3594512.3594527. URL  
719 <https://dl.acm.org/doi/10.14778/3594512.3594527>.

720

721

722

723

724

725

726

727

728

729

730

731

732

733

734

735

736

737

738

739

740

741

742

743

744

745

746

747

748

749

750

751

752

753

754

755

## APPENDIX

**Roadmap.** In Section A, we provide more preliminaries regarding notations and inequalities used throughout the paper. In Section B, we show how to obtain a multiplicative-additive approximation for hitting time given an additive Frobenius norm approximation of the Laplacian. In Section C, we provide missing proofs for prior statements. In Section D, we supply more details for HNSW data structure. In Section E, we present more details about experiments in Section 5 and an extra set of experiments in the steady state setting.

## A MORE PRELIMINARIES

## A.1 NOTATIONS

Let  $n$  be a natural number, we use  $[n]$  to denote the set  $\{1, 2, \dots, n\}$ . Let  $X$  be a random variable, we use  $\mathbb{E}[X]$  to denote the expectation of  $X$ , and let  $E$  be an event, we use  $\Pr[E]$  to denote the probability that event  $E$  happens.

Let  $G = (V, E, w)$  be a graph where  $V$  is the set of vertices,  $E$  is the set of edges and  $w : E \rightarrow \mathbb{R}_+$  be the weight function that assigns a positive real number to each edge. We adopt the convention and let  $n := |V|$  and  $m := |E|$ . Given a vertex  $u \in V$ , we use  $N(u)$  to denote its neighborhood, i.e.,  $N(u) = \{v \in V : \{u, v\} \in E\}$ .

Let  $x \in \mathbb{R}^d$ , without specification, we use  $\|x\|$  to denote a general norm of  $x$ , we use  $\|x\|_2$  to denote the  $\ell_2$  or Euclidean norm of  $x$ . Let  $M \in \mathbb{R}^{n \times d}$  be a matrix, we use  $\|M\|$  to denote the spectral norm of  $M$ ,  $\|M\|_F$  to denote its Frobenius norm. We use  $M^\dagger$  to denote the pseudo-inverse of matrix  $M$ . If  $M \in \mathbb{R}^{n \times n}$  and is real, symmetric, we use  $\lambda_1(M), \dots, \lambda_n(M)$  to denote its eigenvalues, ordered in ascending order. When  $M$  is clear from context, we use  $\lambda_1, \dots, \lambda_n$  to denote these eigenvalues. We use  $\text{tr}[M]$  to denote the trace of  $M$ , i.e.,  $\text{tr}[M] = \sum_{i=1}^n M_{i,i}$ .

## A.2 USEFUL INEQUALITIES

We collect some useful inequalities to be used later.

**Lemma A.1** (Markov's inequality). *Let  $X$  be a non-negative random variable and  $a > 0$ , then*

$$\Pr[X > a \cdot \mathbb{E}[X]] \leq \frac{1}{a}.$$

**Lemma A.2** (Weyl's inequality, Weyl (1912)). *Let  $A, B \in \mathbb{R}^{n \times n}$  be symmetric matrices, then for any  $i \in [n]$ ,*

$$|\lambda_i(A) - \lambda_i(B)| \leq \|A - B\|.$$

**Lemma A.3** (Theorem 4.1 of Wedin (1973)). *For two conforming matrices  $A, B$ ,*

$$\|A^\dagger - B^\dagger\| \leq 2 \cdot \max\{\|A^\dagger\|^2, \|B^\dagger\|^2\} \cdot \|A - B\|.$$

## B HITTING TIME AND MULTIPLICATIVE-ADDITIONAL APPROXIMATION

In this section, we prove that if we can generate a matrix  $L'$  with  $\|L' - L\|_F \leq \delta$ , then the hitting time can be also approximated in a multiplicative-additive error manner. We first introduce effective resistance, an important metric on graphs that could be associated with the graph Laplacian matrix.

**Definition B.1.** *Let  $G = (V, E, w)$  be a graph and  $u, v \in V$ , the effective resistance between  $u$  and  $v$ , denoted by  $R_G(u, v)$ , is defined as*

$$R_G(u, v) = \chi_{u,v}^\top L^\dagger \chi_{u,v},$$

where  $\chi_{u,v} = e_u - e_v$ .

Tetali (Tetali, 1991) proves that hitting time and effective resistance are intrinsically connected as follows.

810  
 811 **Lemma B.2** (Theorem 5 of Tetali (1991)). *Let  $G = (V, E, w)$  be a graph and  $u, v \in V$  with  $u \neq v$ , the hitting time and effective resistance obeys the following identity:*

812  
 813 
$$h(u, v) = \frac{1}{2} \sum_{z \in V} \deg(z)(R_G(u, v) + R_G(v, z) - R_G(u, z)).$$
  
 814  
 815

816 We need to define the edge expansion of a graph, as we will use Cheeger's inequality to lower bound  
 817 the smallest nontrivial eigenvalue of the Laplacian matrix.

818 **Definition B.3** (Edge expansion). *Let  $G = (V, E, w)$  be a graph and  $S \subseteq V$ , define  $e(S) =$   
 819  $\sum_{u \sim v, u \in S, v \in V \setminus S} w(u, v)$ , the edge expansion of a set  $S$  is defined as*

820  
 821 
$$\phi(S) = \frac{e(S)}{\min\{|S|, |V \setminus S|\}},$$
  
 822

823 the edge expansion of the graph  $G$  is defined as

824  
 825 
$$\phi(G) = \min_{S \subseteq V} \phi(S).$$
  
 826

827 Cheeger's inequality gives a lower bound on  $\lambda_2(L)$  in terms of edge expansion.

828 **Lemma B.4** (Cheeger's inequality, Cheeger (1971)). *Let  $G = (V, E, w)$  be a graph and  $\phi(G)$   
 829 be the edge expansion of  $G$  (Definition B.3). Let  $\lambda_2$  be the second smallest eigenvalue of  $L$  and  
 830  $d_{\max} = \max_{u \in V} \deg(u)$ , then*

831  
 832 
$$\frac{\phi(G)^2}{2d_{\max}} \leq \lambda_2 \leq 2\phi(G).$$
  
 833

834 We next prove that if  $\|L - L'\|_F \leq \delta$ , then  $\|L^\dagger - (L')^\dagger\|$  can also be bounded by invoking Lemma A.3.

835 **Lemma B.5.** *Let  $G = (V, E, w)$  be a graph and  $L$  be its corresponding Laplacian matrix, let  
 836  $G' = (V, E', w')$  be the graph where  $E' \subseteq E$ ,  $L'$  be its Laplacian matrix and  $G'$  is connected.  
 837 Suppose  $\|L - L'\|_F \leq \delta$  for some  $\delta > 0$ , then*

838  
 839 
$$\|L^\dagger - (L')^\dagger\| \leq 2\delta \left( \frac{\phi(G)^2}{2d_{\max}} - \delta \right)^{-2},$$
  
 840

841 where  $\phi(G)$  is the edge expansion of  $G$  (Definition B.3) and  $d_{\max}$  is the max degree of  $G$ .

843 *Proof.* The proof will be combining Lemma A.3 and Lemma B.4. By Lemma A.3, we have

844  
 845 
$$\|L^\dagger - (L')^\dagger\| \leq 2 \cdot \max\{\|L^\dagger\|^2, \|(L')^\dagger\|^2\} \cdot \|L - L'\|,$$
  
 846

847 where we already have

848  
 849 
$$\|L - L'\| \leq \|L - L'\|_F \leq \delta,$$
  
 850

851 meanwhile, by Weyl's inequality (Lemma A.2), this also implies a bound on  $\lambda_2(L')$ :

852  
 853 
$$|\lambda_2(L) - \lambda_2(L')| \leq \|L - L'\| \leq \delta,$$
  
 854

855 it remains to establish a bound on  $\lambda_2(L)$ . By Cheeger's inequality, we obtain

856  
 857 
$$\lambda_2(L) \geq \frac{\phi(G)^2}{2d_{\max}},$$
  
 858

859 since  $L$  has rank  $n - 1$ , we know that

860  
 861 
$$\|L^\dagger\| = \frac{1}{\lambda_2(L)}$$
  
 862 
$$\leq \frac{2d_{\max}}{\phi(G)^2},$$
  
 863

864 similarly we can attempt to establish a bound on  $\lambda_2(L')$ :

865  
 866 
$$\lambda_2(L) - \delta \leq \lambda_2(L') \leq \lambda_2(L) + \delta,$$
  
 867

864 therefore

$$866 \quad \lambda_2(L') \geq \frac{\phi(G)^2}{2d_{\max}} - \delta$$

868 and by the same argument as  $\|L^\dagger\|$ ,

$$870 \quad \|(L')^\dagger\| = \frac{1}{\lambda_2(L')}$$

$$871 \quad \leq \frac{2d_{\max}}{\phi(G)^2 - 2d_{\max}\delta},$$

874 we conclude the following bound:

$$876 \quad \max\{\|L^\dagger\|^2, \|(L')^\dagger\|^2\} \leq \left(\frac{\phi(G)^2}{2d_{\max}} - \delta\right)^{-2}.$$

879 Put things together, we obtain the final bound:

$$880 \quad \|L^\dagger - (L')^\dagger\| \leq 2\delta \left(\frac{\phi(G)^2}{2d_{\max}} - \delta\right)^{-2}. \quad \square$$

883 As a natural corollary, we also obtain a bound on the effective resistance.

884 **Corollary B.6.** *Let  $G = (V, E, w)$  be a graph and  $G' = (V, E', w')$  with  $E' \subseteq E$ ,  $L'$  be its*

885 *Laplacian matrix and  $G'$  is connected. Suppose  $\|L - L'\|_F \leq \delta$  for some  $\delta > 0$ , then for any*

886  *$u, v \in V$ ,*

$$888 \quad |R_G(u, v) - R_{G'}(u, v)| \leq 4\delta \left(\frac{\phi(G)^2}{2d_{\max}} - \delta\right)^{-2}.$$

891 *Proof.* Fix  $u, v \in V$ , then

$$892 \quad |\chi_{u,v}^\top (L^\dagger - (L')^\dagger) \chi_{u,v}| \leq \|L^\dagger - (L')^\dagger\| \cdot \|\chi_{u,v}\|_2^2$$

$$893 \quad \leq 4\delta \left(\frac{\phi(G)^2}{2d_{\max}} - \delta\right)^{-2},$$

896 where the last step is by invoking the bound on  $\|L^\dagger - (L')^\dagger\|$  of Lemma B.5.  $\square$

898 It would also be useful to have a handle on the degree.

900 **Corollary B.7.** *Let  $G = (V, E, w)$  be a graph and  $G' = (V, E', w')$  with  $E' \subseteq E$ ,  $L'$  be its*

901 *Laplacian matrix and  $G'$  is connected. Suppose  $\|L - L'\|_F \leq \delta$  for some  $\delta > 0$ , then for any  $u \in V$ ,*

$$902 \quad |\deg_G(u) - \deg_{G'}(u)| \leq \delta.$$

904 *Proof.* Note that  $\deg_G(u) = e_u^\top L e_u$  and  $\deg_{G'}(u) = e_u^\top L' e_u$ , thus

$$906 \quad |\deg_G(u) - \deg_{G'}(u)| = |e_u^\top (L - L') e_u|$$

$$907 \quad \leq \|L - L'\| \cdot \|e_u\|_2^2$$

$$908 \quad = \|L - L'\|$$

$$909 \quad \leq \delta. \quad \square$$

911 We are in the position to prove our main theorem regarding hitting time.

913 **Theorem B.8.** *Let  $G = (V, E, w)$  be a graph and  $G' = (V, E', w')$  with  $E' \subseteq E$ ,  $L'$  be its*

914 *Laplacian matrix and  $G'$  is connected. Suppose  $\|L - L'\|_F \leq \delta$  for some  $\delta > 0$ , then for any  $u, v \in V$  with*

915  *$u \neq v$ ,*

$$916 \quad |h_G(u, v) - h_{G'}(u, v)| \leq \frac{\delta}{d_{\min}} h_G(u, v) + 12\delta \left(\frac{\phi(G)^2}{2d_{\max}} - \delta\right)^{-2} \sum_{e \in E} w_e$$

918 *Proof.* By Lemma B.2, we know that  
 919

$$920 \quad h_G(u, v) = \frac{1}{2} \sum_{z \in V} \deg_G(z)(R_G(u, v) + R_G(v, z) - R_G(u, z)), \quad (1)$$

922 by Corollary B.6, we have that  
 923

$$924 \quad |R_G(u, v) - R_{G'}(u, v)| \leq 4\delta \left( \frac{\phi(G)^2}{2d_{\max}} - \delta \right)^{-2},$$

927 for ease of notation, let  $\delta' := 4\delta \left( \frac{\phi(G)^2}{2d_{\max}} - \delta \right)^{-2}$ , and by Corollary B.7,  
 928

$$929 \quad |\deg_G(u) - \deg_{G'}(u)| \leq \delta.$$

930 To apply Eq. (1), we examine one term as follows:  
 931

$$932 \quad \begin{aligned} \deg_G(z)R_G(u, v) - \deg_{G'}(z)R_{G'}(u, v) &\leq \deg_G(z)R_G(u, v) - (\deg_G(z) - \delta)R_{G'}(u, v) \\ 933 \quad &\leq \deg_G(z)R_G(u, v) - (\deg_G(z) - \delta)(R_G(u, v) - \delta') \\ 934 \quad &= \delta' \deg_G(z) + \delta R_G(u, v) - \delta \delta' \\ 935 \quad &\leq \delta' \deg_G(z) + \delta R_G(u, v) \end{aligned}$$

937 Putting it together yields  
 938

$$939 \quad \begin{aligned} h_G(u, v) - h_{G'}(u, v) &= \frac{1}{2} \sum_{z \in V} (\deg_G(z)(R_G(u, v) + R_G(v, z) - R_G(u, z)) - \deg_{G'}(z)(R_{G'}(u, v) + R_{G'}(v, z) - R_{G'}(u, z))) \\ 940 \quad &\leq \frac{1}{2} \sum_{z \in V} 3\delta' \deg_G(z) + \delta(R_G(u, v) + R_G(v, z) - R_G(u, z)) \\ 941 \quad &= \frac{3}{2} \delta' \sum_{z \in V} \deg_G(z) + \frac{1}{2} \delta \sum_{z \in V} R_G(u, v) + R_G(v, z) - R_G(u, z) \\ 942 \quad &\leq \frac{3}{2} \delta' \sum_{z \in V} \deg_G(z) + \frac{1}{2} \delta \sum_{z \in V} \deg_G(z)(R_G(u, v) + R_G(v, z) - R_G(u, z)) \cdot \frac{1}{\deg_G(z)} \\ 943 \quad &\leq \frac{3}{2} \delta' \sum_{z \in V} \deg_G(z) + \frac{1}{2} \delta \left( \sum_{z \in V} \deg_G(z)(R_G(u, v) + R_G(v, z) - R_G(u, z)) \right) \cdot \frac{1}{d_{\min}} \\ 944 \quad &= 3\delta' \sum_{e \in E} w_e + \frac{\delta}{d_{\min}} h_G(u, v), \end{aligned}$$

945 this completes the proof.  $\square$   
 946

## 947 C MISSING PROOFS

948 In this section, we include the missing proofs in previous sections.  
 949

950 **Theorem C.1** (Restatement of Theorem 3.1). *Let  $P \subset \mathbb{R}^d$  be an  $n$ -point dataset and  $p \in P$  be a  
 951 point to-be-deleted. Suppose  $P$  is preprocessed by an HNSW data structure and  $p$  is not the entry  
 952 point of the HNSW. Fix a query point  $q \in \mathbb{R}^d$  and suppose the search reaches layer  $l \in \{1, \dots, L\}$ , let  
 953  $N(p)$  denote the neighborhood of  $p$  at layer  $l$ . Suppose  $q$  reaches  $N(p)$ , visits and leaves  $p$ . Consider  
 954 the deletion procedure that removes  $p$  at layer  $l$  and forms a clique over  $N(p)$ , then the search of  $q$   
 955 on the new graph is equivalent to the search of  $q$  on the old graph.*

956 *Proof.* Let  $G$  denote the graph at layer  $l$  before deleting  $p$  and  $G_{\setminus p}$  denote the graph at layer  $l$  after  
 957 deleting  $p$ . By assumption, there is some vertex  $a \in N(p)$  visited by the walk immediately before  
 958 visiting  $p$ , and another vertex  $b \in N(p)$  visited immediately after. We focus our attention on how the  
 959 graph transformation affects the  $a \rightarrow p \rightarrow b$  section of the traversal. In the original graph, the walk  
 960 transitioned from  $a$  to  $p$  because  $p$  is the vector in  $N(a)$  nearest to  $q$ . However, since the walk then

972 transitions from  $p$  to  $b$ , it must be the case that  $b$  is closer to  $q$  than is any point in  $N(p) \cup \{p\}$ , and  
 973 thus  $\|b - q\| = \min_{c \in N(p)} \|c - q\| \leq \|p - q\|$ .  
 974

975 Now, consider the new graph where  $p$  is deleted and a clique is instead inserted between the vectors  
 976 in its former neighborhood. The walk remains the same until it first hits  $a$ . From  $a$ , there are two  
 977 possible (not mutually-exclusive) types of neighbors the walk could transition to: those that were  
 978 neighbors of  $a$  in the original graph, and those new neighbors it acquired when the clique was  
 979 inserted on  $N(p)$ , including  $b$ . Because the old walk transitioned into  $p$ , it must be the case that  
 980  $\|p - q\| \leq \|x - q\|$  for each  $x$  among the original  $N(a)$ . Combining this with the previous inequality,  
 981 it must be the case that  $\|b - q\| = \min_y \|y - q\|$ , with  $y$  ranging over the entire new neighborhood of  
 982  $a$ , and thus the walk must still transition into  $b$ , at which point it proceeds as before.  $\square$   
 983

984 **Theorem C.2** (Restatement of Theorem 4.1). *Let  $G = (V, E, w)$  be a weighted graph, define the  
 985 random walk under the weights  $w$  for any edge  $\{u, v\} \in E$  as  $\Pr[u \rightarrow v | w] = \frac{w(u, v)}{\deg(u)}$  where  
 986  $\deg(u) = \sum_{z \in N(u)} w(u, z)$ . Let  $p$  be the point to be deleted as for any  $u, v \in N(p)$ , define the  
 987 new weights  $w'(u, v)$  as  $w'(u, v) = w(u, v) + \frac{w(u, p) \cdot w(p, v)}{\deg(p)}$ , let  $E(p) = \{\{u, p\} : u \in N(p)\}$  and  
 988  $C(p) = \{\{u, v\} : u \neq v, u, v \in N(p)\}$ , then for the new graph  $G' = (V \setminus \{p\}, E \setminus E(p) \cup C(p), w')$ ,  
 989 we have*

$$\Pr[u \rightarrow v | w'] = \Pr[(u \rightarrow p \rightarrow v) \vee (u \rightarrow v) | w].$$

990  
 991 *Proof.* Consider the neighborhood of  $p$ ,  $N(p)$ , let  $u, v \in N(p)$ , we reason over the probability that  
 992 the walk moves from  $u$  to  $v$ . Note that after deletion, the only change is that the vertex  $p$  has been  
 993 removed from the graph, therefore, there is no path from  $u \rightarrow p \rightarrow v$ . On the other hand, there is  
 994 now a direct path from  $u$  to  $v$  under the new weight  $w'(u, v)$ , so we need to show that the probability  
 995 is not affected.

996 Recall that for any vertex  $z \in N(u)$ , we have that the probability the walk moves from  $u$  to  $z$  is  
 997

$$\frac{w(u, z)}{\deg(u)}$$

1000 where  $\deg(u) = \sum_{z \in N(u)} w(u, z)$ . Before deleting  $p$ , we calculate the probability of the path  
 1001  $u \rightarrow p \rightarrow v$  together with the probability of  $u \rightarrow v$ :

$$\begin{aligned} & \Pr[(u \rightarrow p \rightarrow v) \vee (u \rightarrow v) | w] \\ &= \Pr[u \rightarrow p | w] \cdot \Pr[p \rightarrow v | u \rightarrow p, w] + \Pr[u \rightarrow v | w] \\ &= \frac{w(u, p)}{\deg(u)} \cdot \frac{w(p, v)}{\deg(p)} + \frac{w(u, v)}{\deg(u)} \end{aligned}$$

1007 After deletion, the random walk is performed via new weights  $w'$ :

$$\begin{aligned} \Pr[u \rightarrow v | w'] &= \frac{w'(u, v)}{\deg'(u)} \\ &= \frac{w(u, v)}{\deg'(u)} + \frac{w(u, p) \cdot w(p, v)}{\deg(p) \deg'(u)} \end{aligned} \tag{2}$$

1013 note that

$$\begin{aligned} \deg'(u) &= \sum_{v \in N(u) \setminus N(p)} w(u, v) + \sum_{v \in N(p)} w'(u, v) \\ &= \deg(u) - w(u, p) + \sum_{v \in N(p)} \frac{w(u, p) \cdot w(p, v)}{\deg(p)} \\ &= \deg(u) - w(u, p) + w(u, p) \\ &= \deg(u) \end{aligned}$$

1021 therefore

$$(2) = \frac{w(u, v)}{\deg(u)} + \frac{w(u, p) \cdot w(p, v)}{\deg(p) \cdot \deg(u)},$$

1023 which is the same as the probability of walking from  $u$  to  $v$  either via the edge  $\{u, v\}$  or the path  
 1024  $u \rightarrow p \rightarrow v$ .  $\square$

1026 **Theorem C.3** (Restatement of Theorem 4.3). *Let  $G = (V, E, w)$  and  $L \in \mathbb{R}^{n \times n}$  be its graph*  
 1027 *Laplacian matrix. Suppose we generate a matrix  $\tilde{C} \in \mathbb{R}^{s \times n}$  by sampling each row of  $\sqrt{W}B$*   
 1028 *proportional to its squared row norm with  $s = 200\epsilon^{-2}$ , and reweight row  $i$  by  $1/(p_i s)$  where*  
 1029  *$p_i = \|(\sqrt{W}B)_{i,*}\|_2^2 / \|\sqrt{W}B\|_F^2$ , then with probability at least 0.99,*  
 1030

$$1031 \quad \|\tilde{C}^\top \tilde{C} - L\|_F \leq \epsilon \cdot \text{tr}[W].$$

1032  
 1033 *Proof.* For simplicity of notation, we let  $C := \sqrt{W}B$ . Define the random variable  $X_i = \frac{1}{p_i} C_{i,*} C_{i,*}^\top$ ,  
 1034 where  $p_1, \dots, p_m$  are the sampling probabilities of the process, i.e.  $p_i = \|C_{i,*}\|_2^2 / \|C\|_F^2$ . We prove  
 1035 several important properties of these  $X_i$ 's.  
 1036

- Expectation. Note that

$$\begin{aligned} 1039 \quad \mathbb{E}[X] &= \sum_{i=1}^m p_i \cdot \frac{1}{p_i} C_{i,*} C_{i,*}^\top \\ 1040 &= \sum_{i=1}^m C_{i,*} C_{i,*}^\top \\ 1041 &= C^\top C \\ 1042 &= C^\top C \\ 1043 &= C^\top C \\ 1044 &= C^\top C \\ 1045 &= C^\top C \end{aligned}$$

- Expected Frobenius norm. We compute the entrywise variance of  $X$ :

$$\begin{aligned} 1046 \quad \mathbb{E}[\|X\|_F^2] &= \sum_{i,j=1}^n \mathbb{E}[x_{i,j}^2] \\ 1047 &= \left( \sum_{i,j=1}^n \sum_{k=1}^n p_k \frac{1}{p_k^2} \cdot C_{k,i}^2 C_{k,j}^2 \right) \\ 1048 &= \sum_{k=1}^n \frac{1}{p_k} \|C_{k,*}\|_2^4 \\ 1049 &= \|C\|_F^4, \end{aligned}$$

1050 let  $Y = \frac{1}{s} \sum_{i=1}^s X_i$ , then

$$\begin{aligned} 1051 \quad \mathbb{E}[\|Y\|_F^2] &= \mathbb{E}\left[\left\|\frac{1}{s} \sum_{i=1}^s X_i\right\|_F^2\right] \\ 1052 &= \frac{1}{s^2} \left( \sum_{i=1}^s \mathbb{E}[\|X\|_F^2] + 2 \sum_{i \neq j} \mathbb{E}[\text{tr}[X_i X_j]] \right) \\ 1053 &= \frac{\|C\|_F^4}{s} + \frac{2}{s^2} \sum_{i \neq j} \text{tr}[\mathbb{E}[X_i X_j]] \\ 1054 &= \frac{\|C\|_F^4}{s} + \frac{2}{s^2} \sum_{i \neq j} \text{tr}[\mathbb{E}[X_i] \mathbb{E}[X_j]] \\ 1055 &= \frac{\|C\|_F^4}{s} + \frac{s-1}{s} \|C^\top C\|_F^2. \end{aligned}$$

- Probability. We will be using Markov inequality on  $\|Y - C^\top C\|_F^2$ , to do so we first compute

$$\begin{aligned} 1078 \quad \mathbb{E}[\text{tr}[Y C^\top C]] &= \text{tr}[\mathbb{E}[Y C^\top C]] \\ 1079 &= \text{tr}[\mathbb{E}[Y] C^\top C] \end{aligned}$$

$$= \text{tr}[C^\top C C^\top C] \\ = \|C^\top C\|_F^2,$$

and we can compute the expectation of the squared Frobenius norm deviation:

$$\begin{aligned} & \mathbb{E}[\|Y - C^\top C\|_F^2] \\ &= \mathbb{E}[\|Y\|_F^2] + \|C^\top C\|_F^2 - 2\mathbb{E}[\text{tr}[YC^\top C]] \\ &= \frac{\|C\|_F^4}{s} + \frac{2s-1}{s}\|C^\top C\|_F^2 - 2\|C^\top C\|_F^2 \\ &\leq \frac{\|C\|_F^4}{s}. \end{aligned}$$

Set  $s = 100\epsilon^{-2}$ , we obtain that  $\mathbb{E}[\|Y - C^\top C\|_F^2] \leq \epsilon^2\|C\|_F^4$ . By Markov's inequality (Lemma A.1), we have

$$\Pr[\|Y - C^\top C\|_F^2 > \epsilon^2\|C\|_F^4] \leq \frac{\epsilon^2/100 \cdot \|C\|_F^4}{\epsilon^2\|C\|_F^4} = \frac{1}{100},$$

as desired. Utilizing the structure of  $C$ , we could further simplify the bound:  $\|C\|_F^2 = 2 \sum_{e \in E} w_e = 2\|w\|_1 = 2\text{tr}[W]$ .  $\square$

**Corollary C.4** (Restatement of Corollary 4.6). *Let  $G = (V, E, w)$  be a weighted complete graph and  $G' = (V, E', w')$  be the induced graph by applying Theorem 4.3 to  $G$ , and assume  $G'$  is connected. If  $|E'| = O(\max_{u,v \in N(p)} h_G(u,v) \cdot n)$ , then with probability at least 0.99, for any  $u, v \in V$ ,  $|h_G(u,v) - h_{G'}(u,v)| \leq \sqrt{n \cdot h_G(u,v)}$ . given one of the two settings:*

- *Single cluster: for any  $u, v \in V$ ,  $w(u,v) = O(1)$ ;*
- *Many small clusters: there are  $\sqrt{n}$  clusters of size  $\sqrt{n}$ . Within each cluster, the edge weights are  $O(1)$ , and between clusters, the edge weights are  $O(1/n)$ .*

*Proof.* We prove the two settings item by item.

- Single cluster, that is, for all  $u, v, u', v' \in V$ , we have  $w(u,v) = O(w(u',v')) = O(1)$ . In this case,  $\text{tr}[W] = O(n^2)$ ,  $d_{\min}, d_{\max} = O(n)$  and  $\phi(G) = O(n)$ . The multiplicative error factor for  $h_G(u,v)$  is then  $\epsilon \cdot n$  and the additive error term is  $\epsilon \cdot n^4(n - \epsilon \cdot n^2)^{-2} = \frac{\epsilon n^2}{(1-\epsilon n)^2} \leq 4\epsilon^{-1}$ , so the overall error is  $\epsilon n \cdot h_G(u,v) + 4\epsilon^{-1}$ , equating these two terms sets  $\epsilon^{-1} = \sqrt{n \cdot h_G(u,v)}$ . According to Theorem 4.3, this means that we can sparsify the number of edges in clique  $C(p)$  from  $O(|N(p)|^2)$  down to  $O(\max_{u,v \in N(p)} h(u,v) \cdot |N(p)|)$ .
- Many small clusters, in particular the max edge weight is  $O(1)$  while the min edge weight is  $O(n^{-1})$ . Among the  $n$  points, we assume they are clustered  $n^{0.5}$  parts, each of size  $n^{0.5}$ . For the  $O(n^2)$  intercluster edges, the edge weights are  $O(n^{-1})$ , while other edges have weights  $O(1)$ . In this case,  $\text{tr}[W] = n + n^{1.5} \leq O(n^{1.5})$ ,  $d_{\min}, d_{\max} = O(n^{0.5})$  and  $\phi(G) = O(1)$ , and the multiplicative factor is  $\epsilon \cdot n$  and the additive factor is  $\epsilon \cdot n^3(n^{-0.5} - \epsilon \cdot n^{1.5})^{-2} = \frac{\epsilon n^4}{(1-\epsilon n^2)^2} \leq 4\epsilon^{-1}$ , so the overall error is  $\epsilon n \cdot h_G(u,v) + 4\epsilon^{-1}$ . We would set  $\epsilon^{-1} = \sqrt{n \cdot h_G(u,v)}$  to minimize the error. Note that now the number of edges in the sparsified graph is  $O(\max_{u,v \in N(p)} h(u,v) \cdot |N(p)|)$ .  $\square$

## D HNSW DATA STRUCTURE

We review the both classical HNSW data structure proposed in Malkov & Yashunin (2020), also provide more details about our random walk-based variant of it in this section.

### D.1 CLASSICAL HNSW

In this section, we provide a more in-depth review of the HNSW data structure. We lay out its structure in several algorithms, starting from the search procedure.

To construct the HNSW data structure, we implement the insertion procedure.

The insertion works as follows: it simply performs Algorithm 2 from  $L$  to  $l + 1$  where  $l$  is the designated layer for  $q$  to be inserted. Starting from layer  $l$  to 1, we increase the number of points to be returned by Algorithm 2 (efConstruction can be much larger  $m$ ) and then select  $m$  of them to add edges using NEIGHBORSELECT. This procedure is then repeated for the new neighbors of  $q$  to prune edges.

The only missing piece is the neighbor selection procedure. [Malkov & Yashunin \(2020\)](#) recommends two types of neighbor selection: one is simply taking the top- $m$  nearest neighbors, while the other involves a more sophisticated heuristic procedure. We refer readers to [Malkov & Yashunin \(2020\)](#) for more details.

## D.2 PROBABILISTIC HNSW

Inspired by the classical HNSW data structure, we propose a random walk-based approach for both searching and constructing the data structure. While we give an overview in Section 4, here we provide the complete algorithm.

The key distinction between Algorithm 2 and 4 is on line 7: instead of taking the nearest neighbor, Algorithm 4 samples a point to move to based on the softmax of negative squared distance. For insertion, we give an alternative presentation that shows how to construct the one layer of HNSW by first building a complete graph, then randomly sparsifying it. It is showcased in Algorithm 5 and Figure 3.

---

1188 **Algorithm 3** HNSW algorithm: insertion.

---

1189 1: **procedure** INSERT( $q \in \mathbb{R}^d, P \subset \mathbb{R}^d, u \in P, \text{efConstruction} \in [|P|], m \in [|P|], m_{\max} \in [|P|]$ )  
1190 2:    $l \leftarrow \lfloor -\ln(\text{Unif}(0, 1)) / \ln m \rfloor$   
1191 3:   **for**  $l_c = L \rightarrow l + 1$  **do**  
1192 4:     candidates  $\leftarrow \text{LAYERSEARCH}(q, P, l_c, u, 1)$   
1193 5:      $u \leftarrow \arg \min_{v \in \text{candidates}} \|v - q\|$   
1194 6:   **end for**  
1195 7:   **for**  $l_c = \min\{L, l\} \rightarrow 1$  **do**  
1196 8:     candidates  $\leftarrow \text{LAYERSEARCH}(q, P, l_c, u, \text{efConstruction})$   
1197 9:     nbrs  $\leftarrow \text{NEIGHBORSELECT}(q, \text{candidates}, m, l_c)$   
1198 10:    Add edges between  $q$  and nbrs at layer  $l_c$   
1199 11:   **end for**  
1200 12:   **for**  $v \in \text{nbrs}$  **do**  
1201 13:      $N(v) \leftarrow \text{nbrhood}(v)$  at layer  $l_c$   
1202 14:     **if**  $|N(v)| > m_{\max}$  **then**  
1203 15:       newNbrs  $\leftarrow \text{NEIGHBORSELECT}(v, N(v), m_{\max}, l_c)$   
1204 16:       Add edges between  $v$  and newNbrs at layer  $l_c$   
1205 17:     **end if**  
1206 18:   **end for**  
1207 19:    $u \leftarrow \text{candidates}$   
1208 20:   **if**  $l > L$  **then**  
1209 21:      $u \leftarrow q$   
1210 22:   **end if**  
1211 23: **end procedure**

---

### D.3 RUNTIME ANALYSIS OF SPATCH

We provide a preliminary runtime analysis of SPatch (Algorithm 1). Let  $p$  be the point we want to delete, then note that the most expensive operation is to compute and update  $w'(u, v)$ , which takes  $O(|N_{\text{in}}(p)| \cdot |N_{\text{out}}(p)| \cdot d)$  time, all other operations are subsumed by this step.

### D.4 CONSTRUCTION VIA SPARSIFICATION

The typical construction process of an HNSW graph involves the following steps:

- Given a point  $u$ , determine the layer  $l_u$  to be inserted;
- Perform greedy search for  $u$  from layer  $L$  down to  $l_u + 1$ , moving a layer downward each time the search is stuck;
- In layers  $l = l_u \dots 1$ , perform a greedy search for  $u$ , and draw edges between  $u$  and the  $m$  nearest points to it that were visited along the search path.

Having replaced greedy search with a softmax walk, we can provide a probabilistic interpretation of the graph construction process as a sparsification of the weighted complete graph, as follows. Let  $G_0$  be a weighted complete graph with the edge weight between two vertices  $u, v$  being  $\exp(-r^2 \cdot \|u - v\|^2)$ . We claim that each layer of the HNSW graph  $G_1$  can be constructed via a random walk-based sparsification of  $G_0$ . To this end, fix an ordering of the vertices  $v_1, \dots, v_n$ , and initialize the graph with a single node  $v_1$ . Then, alternate between the complete graph  $G_0$  and a sparsified graph as follows: for  $i = 2, \dots, n$ ,

- **Densify:** Add  $v_i$  to  $G_1$  by adding all edge  $\{v_i, v_j\}$  for  $j \in [i - 1]$ , with edge weights  $\exp(-r^2 \cdot \|v_i - v_j\|^2)$ .
- **Random walk:** Perform a softmax walk for  $v_i$  in  $G_1$  starting at  $v_1$ , maintaining a list of the nodes visited along the walk.
- **Sparsify:**
  - After the random walk terminates, sample  $m$  points from visited with probability proportional to the edge weights attached to them in the Densify step, forming a set sample. Remove edges between  $v_i$  and points not in sample.

---

**Algorithm 4** HNSW algorithm: layer search.

---

```

1244 1: procedure LAYERSEARCHRANDOMWALK( $q \in \mathbb{R}^d, P \subset \mathbb{R}^d, l \in \{0, \dots, L\}, u \in P, m \in$ 
1245  $\llbracket P \rrbracket, r \in \mathbb{R}_+$ )
1246 2:    $\triangleright l$  is the layer of the graph,  $u$  is the starting point and  $m$  is the total number of nearest
1247   neighbors to return.
1248 3:    $\text{visited} \leftarrow \{u\}$   $\triangleright$  Visited vertices.
1249 4:    $\text{candidates} \leftarrow \{u\}$   $\triangleright$  Candidate vertices.
1250 5:    $\text{nbrs} \leftarrow \{u\}$   $\triangleright$  Dynamic list of nearest neighbors.
1251 6:   while  $|\text{candidates}| > 0$  do
1252 7:     Sample  $c$  with probability  $\frac{\exp(-r^2 \cdot \|c-q\|^2)}{\sum_{v \in \text{candidates}} \exp(-r^2 \cdot \|v-q\|^2)}$ 
1253 8:      $f \leftarrow$  furthest neighbor of  $q$  in  $\text{nbrs}$ 
1254 9:      $\text{candidates} \leftarrow \text{candidates} \setminus \{c\}$ 
1255 10:    if  $\|c-q\| > \|f-q\|$  then
1256 11:      break
1257 12:    end if
1258 13:    for  $v \in \text{nbrhood}(c)$  at layer  $l$  do
1259 14:      if  $v \notin \text{visited}$  then
1260 15:         $\text{visited} \leftarrow \text{visited} \cup \{v\}$ 
1261 16:         $f \leftarrow$  furthest neighbor of  $q$  in  $\text{nbrs}$ 
1262 17:        if  $\|v-q\| < \|f-q\|$  or  $|\text{nbrs}| < m$  then  $\triangleright$  Either  $v$  is closer or  $\text{nbrs}$  is not
1263 18:           $\text{candidates} \leftarrow \text{candidates} \cup \{v\}$ 
1264 19:           $\text{nbrs} \leftarrow \text{nbrs} \cup \{v\}$ 
1265 20:          if  $|\text{nbrs}| > m$  then
1266 21:            Remove furthest neighbor of  $q$  in  $\text{nbrs}$ 
1267 22:          end if
1268 23:          end if
1269 24:        end if
1270 25:      end for
1271 26:    end while
1272 27:    return  $\text{nbrs}$ 
1273 28: end procedure

```

---

- Sparsify the neighborhood of each  $u \in \text{sample}$  by subsampling  $m$  of the edges incident to  $u$  with probability proportional to their edge weight.

This point of view also justifies our use of edge weights when performing deletion, as we could treat the edge weights are formed during construction and inserting the corresponding the point.

## E ADDITIONAL EXPERIMENTS

## E.1 DETAILS OF PREVIOUS EXPERIMENTS

We start by examining more details regarding prior experiments conducted in Section 5.

**Deletion experiments.** Regarding deletion algorithms, we note that several of them have hyper-parameters:

- FreshDiskANN (Singh et al., 2021) requires a hyper-parameter  $\alpha$ , which governs how many edges to prune after rerouting  $u$  to  $N(p) \cup N(u)$ , intuitively, the larger the  $\alpha$ , the denser the graph. According to Singh et al. (2021),  $\alpha$  should be chosen  $> 1$ . In our experiment, due to the time-consuming nature of FreshDiskANN deletion procedure, we set  $\alpha = 1.2$ . It is also worth noting that FreshDiskANN is designed for DiskANN, which has a slightly different insertion procedure from HNSW.
- Our algorithm `SPatch` also requires a hyper-parameter  $\alpha$ , which determines how many edges to keep in the clique after sparsification. Intuitively, the larger the  $\alpha$ , the denser the graph. Through our experiments, we observe that choosing  $\alpha = 1.2$  except for `GIST` yields good performances. In

---

1296 **Algorithm 5** Construction via sparsification.

---

1297 1: **procedure** CONSTRUCTONELAYER( $P \in (\mathbb{R}^d)^n, m \in [n], r \in \mathbb{R}_+$ )  
1298 2:     Determine an ordering of the points in  $P$ , label them as  $v_1, \dots, v_n$   
1299 3:      $G \leftarrow (\{v_1\}, \emptyset)$   
1300 4:     **for**  $i = 2 \rightarrow n$  **do**  
1301 5:          $\text{candidates} \leftarrow \{v_1\}$   
1302 6:          $\text{visited} \leftarrow \{v_1\}$   
1303 7:          $V \leftarrow V \cup \{v_i\}$   
1304 8:         **// Densify phase**  
1305 9:          $E \leftarrow E \cup \{\{v_j, v_i\} : j \in [i-1], w(v_j, v_i) = \exp(-r^2 \cdot \|v_j - v_i\|^2)\}$   
1306 10:         **// Random walk phase**  
1307 11:         **while**  $|\text{candidates}| > 0$  **do**  
1308 12:             Sample  $c \in \text{candidates}$  with probability  $\frac{\exp(-r^2 \cdot \|v_i - c\|^2)}{\sum_{u \in \text{candidates}} \exp(-r^2 \cdot \|v_i - u\|^2)}$   
1309 13:              $\text{candidates} \leftarrow \text{candidates} \setminus \{c\}$   
1310 14:             **for**  $u \in \text{nbrhood}(c)$  **do**  
1311 15:                 **if**  $u \notin \text{visited}$  **then**  
1312 16:                      $\text{visited} \leftarrow \text{visited} \cup \{u\}$   
1313 17:                      $\text{candidates} \leftarrow \text{candidates} \cup \{u\}$   
1314 18:                 **end if**  
1315 19:             **end for**  
1316 20:         **end while**  
1317 21:         **// Sparsify phase**  
1318 22:         sample  $\leftarrow$  Sample  $m$  points from  $\text{visited}$  independently without replacement, with  
1319         probability of sampling  $u$  being  $\frac{\exp(-r^2 \cdot \|v_i - u\|^2)}{\sum_{v \in \text{visited}} \exp(-r^2 \cdot \|v_i - v\|^2)}$   
1320 23:          $E \leftarrow E \setminus \{\{v_j, u\} : u \notin \text{sample}\}$   
1321 24:         **for**  $u \in \text{sample}$  **do**  
1322 25:             **if**  $\text{deg}(u) > m$  **then**  
1323 26:                 Sparsify  $\text{nbrhood}(u)$  by sampling  $m$  edges  
1324 27:             **end if**  
1325 28:         **end for**  
1326 29:     **end for**  
1327 30: **end procedure**

---

1330 particular, this consistently holds for MPNet and MiniLM. For SIFT, we could further improve  
1331 the recall and efficiency by choosing  $\alpha = 0.6$ . For GIST however, one has to choose  $\alpha$  to be  
1332 smaller than 1 to obtain good recall and efficiency. In our experiment, we choose  $\alpha = 0.4$ . We  
1333 summarize the choices in Table 3. To choose  $\alpha$ , we recommend either using  $\alpha = 1.2$  or  $\alpha = 0.6$ .

---

	SIFT	GIST	MPNet	MiniLM
$\alpha$	0.6	0.4	1.2	1.2

1338 Table 3: Choices of hyper-parameter  $\alpha$  for different datasets.

1339  
1340  
1341 **Random softmax walk vs. greedy search.** For this experiment, we need to choose a hyper-parameter  
1342  $r$  (recall the softmax walk samples for the next visit with probability  $\exp(-r^2 \cdot \|q - u\|^2)$ ). Intuitively,  
1343 we want to choose  $r$  so that the softmax walk samples the nearest neighbor with exponentially  
1344 higher probability than the second nearest neighbor. This could be achieved by choosing  $r$  to be  
1345 arbitrarily large. However, if  $r$  is chosen to be too large, the probability can easily overflow. To  
1346 resolve this issue, we adapt the following approach for computing  $r$ : given a collection of points  
1347 candidates to consider (line 7 of Algorithm 4), we compute the empirical average of the distances  
1348  $\mu = \sum_{u \in \text{candidates}} \frac{\|u - q\|}{|\text{candidates}|}$ , then we set  $r = 15/\mu$ . This scales  $r \cdot \|q - u\|$  to a value between  
1349 10 and 20, and empirically, we observe that this choice of  $r$  can differentiate among the top nearest  
neighbors and henceforth, give similar recall as the greedy search.

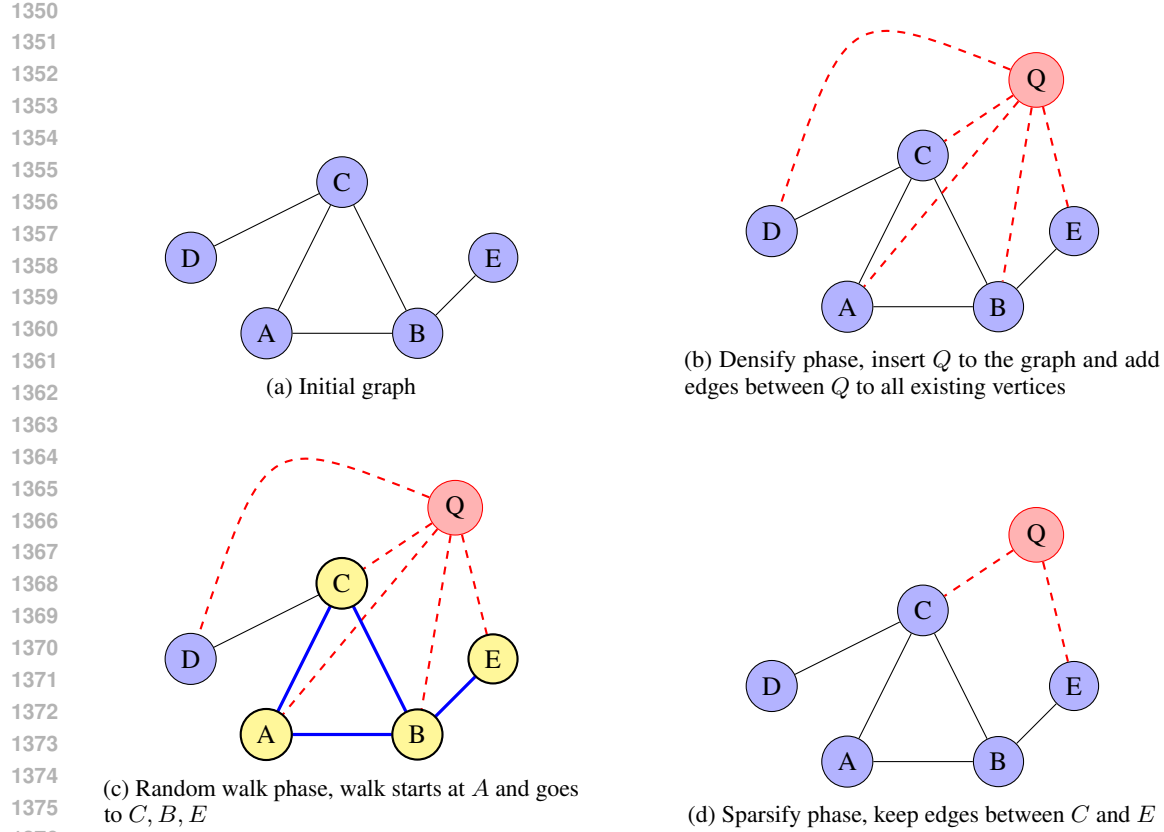


Figure 3: We construct the graph by first adding edges between  $Q$  to all vertices, then perform a random walk to determine the candidate edges to keep, and sparsify them by sampling.

Figure 4 justifies this decision to fix  $r\mu = 15$  by demonstrating the behavior of Random Softmax search for different values  $\hat{r} := r\mu$ . The left plot shows that as  $\hat{r}$  increases, the softmax converges toward a true maximum, and randomized softmax correspondingly better matches the greedy search algorithm. Thus,  $\hat{r}$  in this regime usually – but far from always – transitions to the current node’s neighbor closest to  $q$ . The right plot shows the impact of  $\hat{r}$  on recall, and in particular its convergence to the performance of the pure greedy algorithm (dashed horizontal lines) for  $\hat{r} \approx 15$ . **Deletion time**

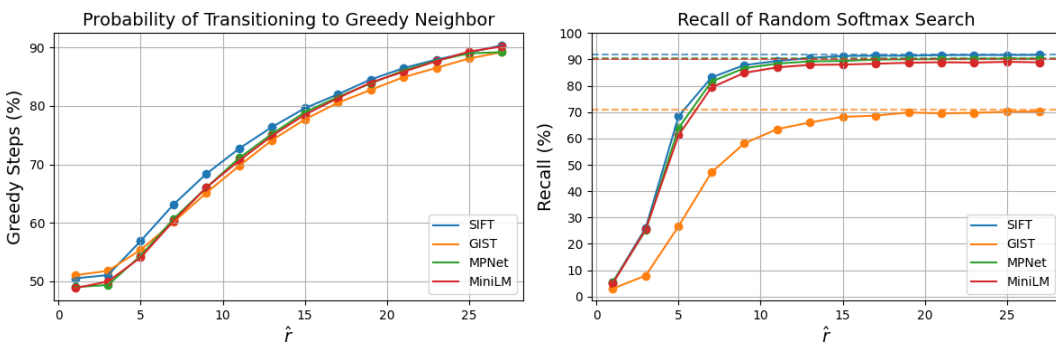


Figure 4: The impact of varying  $\hat{r}$  (i.e.  $r\mu$ ) on transition probabilities and recall. Left: The frequency with which the random softmax algorithm truly transitions to the nearest neighbor (i.e. a greedy step), as a function of  $\hat{r}$ . Right: The impact of different choices of  $\hat{r}$  on the recall of the randomized search algorithm. Horizontal line indicates the recall of greedy search algorithm.

without FreshDiskANN. As we have observed in the experiment, FreshDiskANN has much slower

deletion time than other methods, in the following figures, we provide deletion time comparison *without* FreshDiskANN.

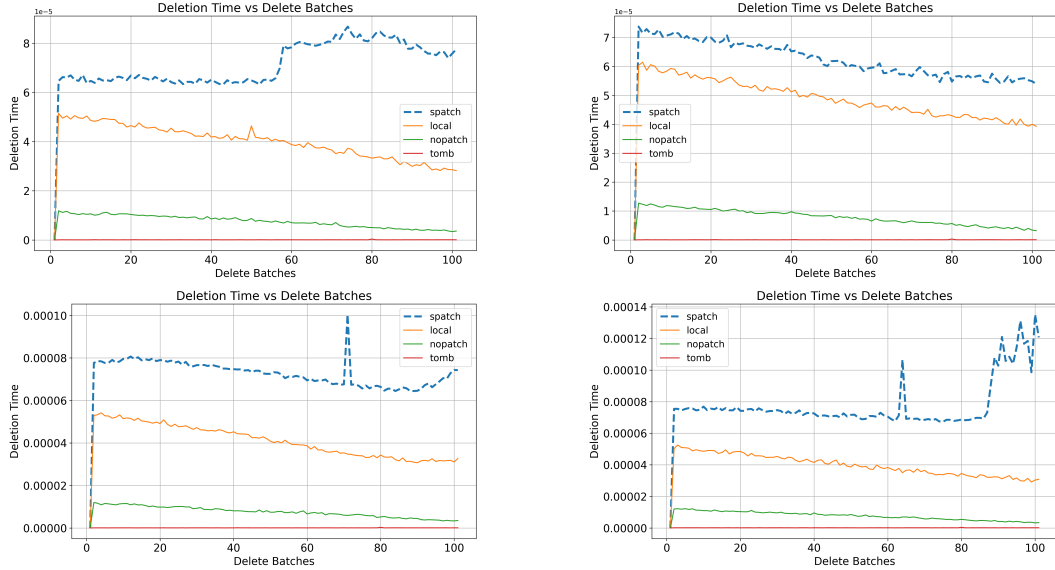


Figure 5: Top left: SIFT, top right: GIST, bottom left: MPNet, bottom right: MiniLM.

## E.2 STEADY STATE SETTING

In this experiment, we consider the steady state setting introduced in Singh et al. (2021), where 10% of the points are deleted from the data structure then inserted back, and queries are measured. We repeat this process 10 times, albeit all points have been deleted from the data structure and reinserted. Similar to the mass deletion experiment, we randomly pick 5,000 query points for SIFT, MPNet, MBREAD and MiniLM and 1,000 query points for GIST.

Through Figure 6, we could see a similar trend as in the deletion experiment (Section 5), except that the no patching algorithm gives better recall than before. This is because in the steady state setting, the graph is automatically ‘‘patched’’ by re-inserting the same set of points back to the data structure. In contrast to the experimental results in Singh et al. (2021), FreshDiskANN does not perform even as well as no patching, this in part is because the insertion algorithms for DiskANN and HNSW are quite different. Regarding hyper-parameters: for FreshDiskANN, we again choose  $\alpha = 1.2$ , and for SPatch, we summarize it in Table 4.

	SIFT	GIST	MPNet	MBREAD	MiniLM
$\alpha$	0.5	0.5	1.2	1.6	1.2

Table 4: Choices of hyper-parameter  $\alpha$  for different datasets.

## E.3 VERTEX COUNTS, EDGE COUNTS, AND MEMORY UTILIZATION

To see the impact of SPatch on the graph size and empirical memory utilization, we design an alternative steady-state experiment in an environment with very high vector turnover. Starting with an empty database, we continuously insert into it one vector per (simulated) second from the MiniLM dataset over the duration of 12 (simulated) hours. Each vector survives for a number of steps following an exponential distribution with a mean of 2 hours (i.e. has a half-life of  $2 \ln 2 \approx 1.39$  hours), after which it is deleted. Hence, while the experiment has more insertions than deletions for the first few simulated hours, it eventually enters a steady state at which insertions and deletions occur at roughly the same rate. At the end of the 12 hours, no new vectors are inserted, and the remaining vectors continue to fall out as they expire.

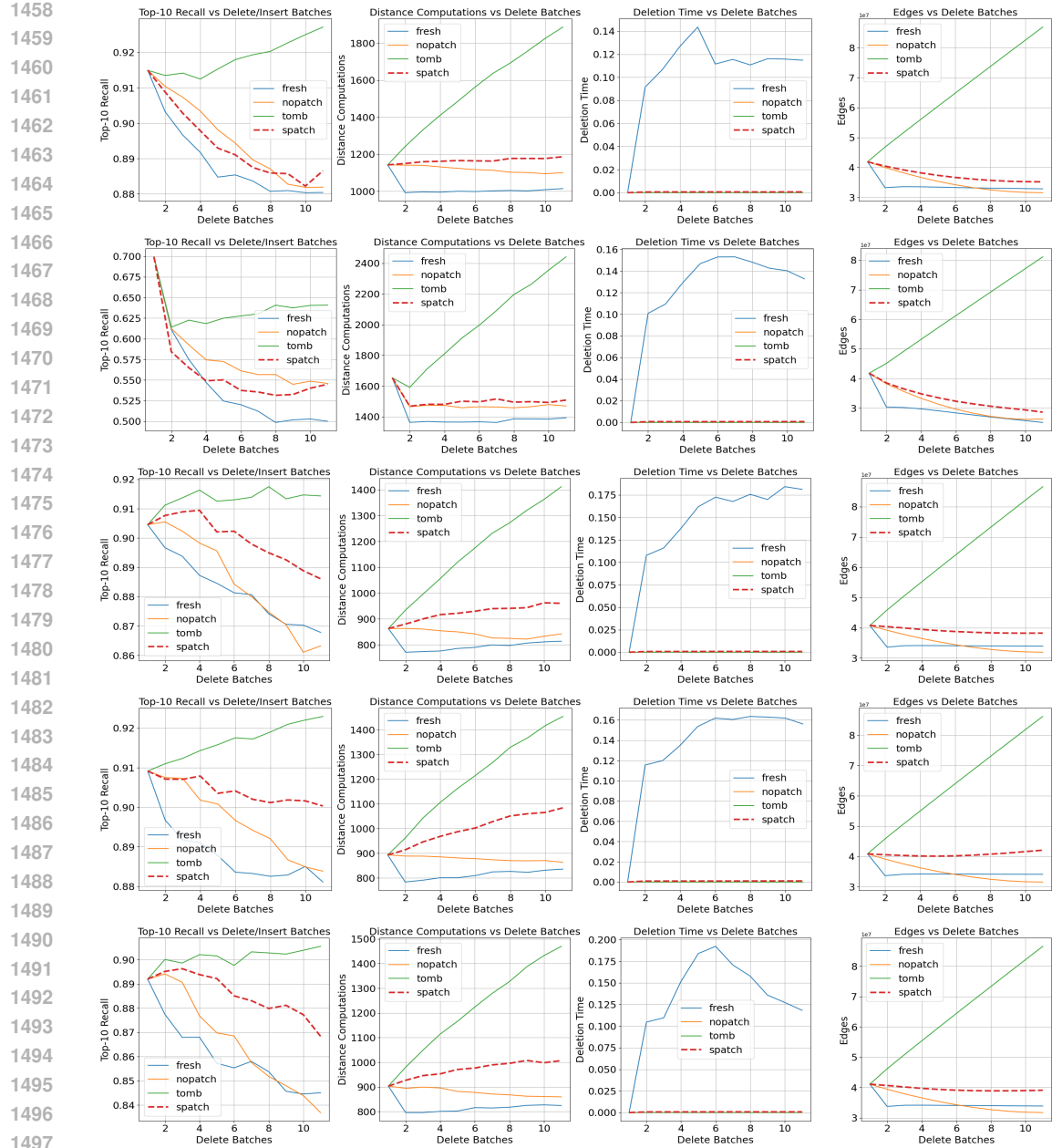


Figure 6: The  $5 \times 4$  grid of figures, where the rows are SIFT, GIST, MPNet, MBREAD and MiniLM, and the columns are recall, number of distance computations per query, total deletion time and total deletion time excluding fresh DiskANN. Legends: spatch – our deletion algorithm SPatch, fresh – FreshDiskANN algorithm, tomb – tombstone algorithm, nopatch – no patching algorithm.

We track the vertex counts, edge counts, and memory utilization of both the Tombstone algorithm and of SPatch, and the results are shown in Figure 7. Vertex and edges are counted cumulatively over all levels of the graph. Hence, we continue to see a small rise even in the steady state: the upper layers of the data structure still continue to accumulate them at their prior rate. However, the rate of increase is *far* slower than that of the Tombstone algorithm, which intrinsically grows at a steady rate independent of the number of deletions.

We also see a stark difference in memory utilization (as measured by python’s `psutil` package). While the `Tombstone` algorithm is marginally more memory efficient before the effect of deletions begins to kick in (as a result of storing approximately  $d + m = 384 + 32 = 416$  words per vector instead of  $d + 2m = 448$  due to the bidirected nature of the HNSW graph), soon the vector deletion begins saving large amounts of memory due to the combined effect of the vertices, edges, and  $d$ -dimensional vectors removed from the data store. Although vertex, edge, and memory all continues to rise with `SPatch`, it does so substantially slower than with `Tombstone`. Finally, after we enter the pure-deletion phase of the experiment 12 hours in, we see no further change in *any* of the plots for `Tombstone` (as expected), but each of the metrics begins its decrease for `SPatch`. While not all of the memory can be directly recovered by the Operating System due to fragmentation or other similar considerations, we do see the memory utilization of `SPatch` begin to dip, and (unlike in `Tombstone`) much of the unrecovered memory is ready for reuse by the algorithm should it face more insertions in the future.

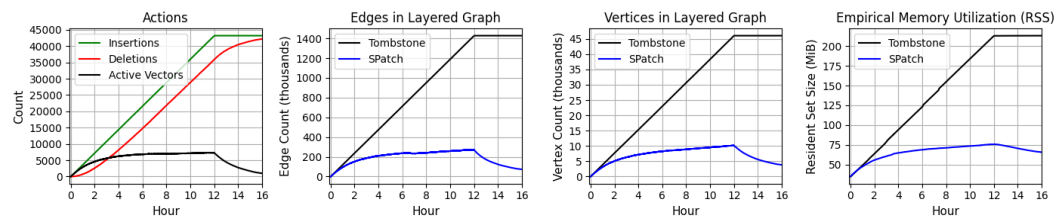


Figure 7: Vertex counts, edge counts, and empirical memory utilization as measured by the experiment described in Section E.3.

#### E.4 SOFTMAX WALK AND GREEDY SEARCH: A MORE DETAILED COMPARISON

In this section, we give a more detailed comparison between softmax walk and greedy search. For the first set of plots, we plot beam size vs recall@10, and for the second set of plots, we plot the total number of distance computations vs recall@10 in Figure 8. We can see that fixing the beam size, softmax walk gives slightly lower recall, but the second row shows that fixing the number of distance computations, softmax walk is very close to greedy search.

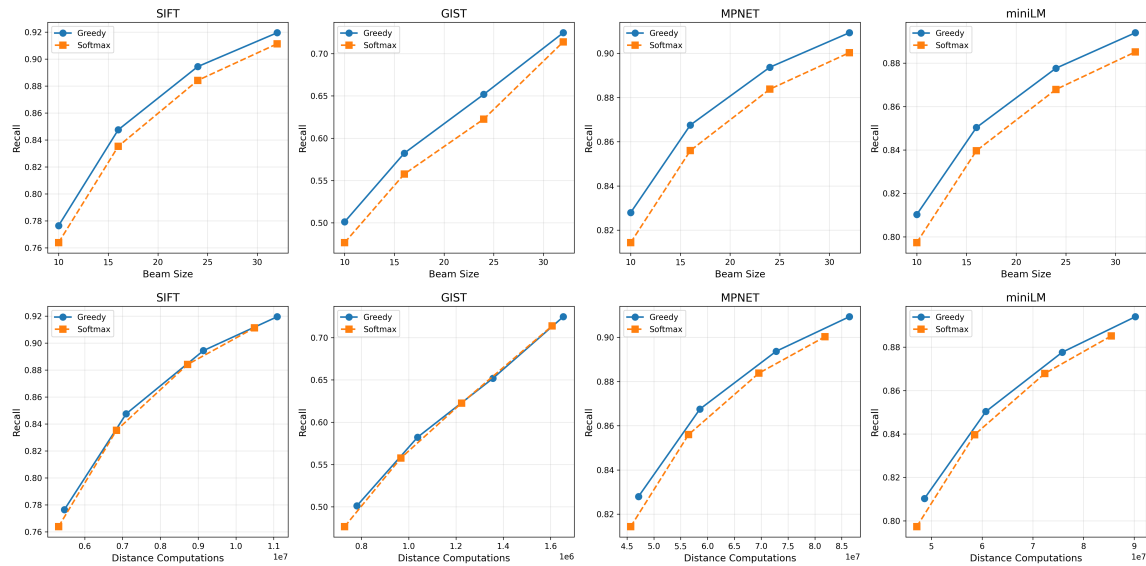


Figure 8: From left to right: SIFT, GIST, MPNet and MiniLM. Top row: beam size vs recall@10, bottom row: total number of distance computations vs recall@10.

1566  
1567

## E.5 EXPERIMENTS ON DISKANN

1568  
1569  
1570  
1571  
1572

In this section, we provide preliminary experiments on DiskANN, specifically we test SPatch, FreshDiskANN, tombstone, local and no patch algorithm. We test it on a subsampled 100k points from SIFT dataset, each deletion batch, we delete 800 points then perform a query. Compared to the experiments on HNSW, FreshDiskANN has improved performance in terms of recall, however, we note the deletion time of FreshDiskANN is still very large.

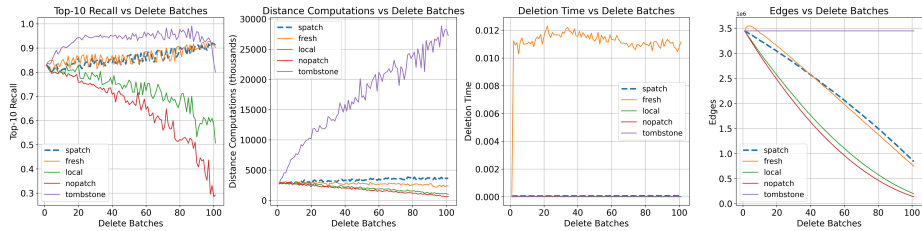
1573  
1574  
1575  
1576  
1577  
1578  
1579  
15801581  
1582

Figure 9: Experiments for DiskANN on 10% of points from SIFT.

1583

1584  
1585

## E.6 EXPERIMENTS ON DYNAMIC EXPLORATION GRAPHS (DEG)

1586  
1587  
1588  
1589  
1590  
1591  
1592

We also provide preliminary comparisons to the deletion strategy used in the Dynamic Exploration Graph (DEG) data structure of Hezel et al. (2025). In DEG, the deletion of a vertex  $v$  is patched by building an independent BFS trees from *each* neighbor of  $v$  and adding an edge between two of these neighbors when their corresponding trees collide, until the total degree on the neighborhood is restored. Like in the previous section, we subsample 100k points from SIFT and monitor (i) recall, (ii) distance computations per query, (iii) deletion time, and (iv) graph size after repeatedly deleting 10K points.

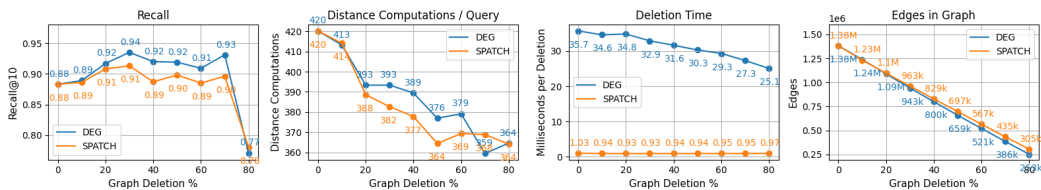
1593  
1594  
1595  
1596  
1597  
1598  
15991600  
1601

Figure 10: Experiments for DEG on 10% of points from SIFT.

1602

The results are shown in Figure 10. Note that DEG’s deletion time is much slower than our method, SPATCH. In the cost/accuracy trade-off, SPatch and DEG perform very similarly, with DEG achieving slightly higher recall (within 2-3%) with a slightly higher number of distance computations, rendering their cost/accuracy tradeoff comparable. The crucial difference is deletion time: **the deletion time of DEG is up to 35x larger than SPatch**, reflecting the inherent cost of DEG’s global rebuild strategy compared to SPatch local updates. This gap makes DEG impractical when deletions are frequent or substantial, which is precisely the regime our method targets. While DEG achieves slightly higher recall than SPatch, its much slower deletion time makes it impractical for use in scenarios where deletions are plentiful.

1611

1612

## LLM DISCLOSURE

1613

1614

This work does not use LLM to facilitate writing.

1615  
1616  
1617  
1618  
1619